| BPDAI | | | | | |
|---|---|---|---|---|---|
| SKIN | ACTIVITY | | ACTIVITY | | DAMAGE |
| Anatomical location | Erosions/Blisters | Number of Lesions if <3 | Urticaria/ Erythema / Other | Number of Lesions if <3 | Pigmentation / Other |
| | 0 absent | | 0 absent | | Absent 0, present 1 |
| | 1 1-3 lesions, none > 1 cm diameter | | 1 1-3 lesions, none >6 cm diameter | | |
| | 2 1-3 lesions, at least one > 1 cm diameter | | 2 1-3 lesions, at least one lesion > 6 cm diameter | | |
| | 3 >3 lesions, none > 2 cm diameter | | 3 >3 lesions, or at least one lesion > 10 cm | | |
| | 5 >3 lesions, and at least one >2 cm | | 5 >3 lesions and at least one lesion > 25 cm | | |
| | 10 >3 lesions, and at least one lesion >5 cm diameter or entire area | | 10 >3 lesions and at least one lesion > 50 cm diameter or entire area | | |
| | | | | | |
| Head | | | | | |
| Neck | | | | | |
| Chest | | | | | |
| Left arm | | | | | |
| Right arm | | | | | |
| Hands | | | | | |
| Abdomen | | | | | |
| Genitals | | | | | |
| Back/Buttocks | | | | | |
| Left leg | | | | | |
| Right leg | | | | | |
| Feet | | | | | |
| Total skin | /120 | | /120 | | |
| MUCOSA | Erosions/Blisters | | | | |
| | 1 1 lesion | | | | |
| | 2 2-3 lesions | | | | |
| | 5 >3 lesions, or 2 lesions >2cm | | | | |
| | 10 entire area | | | | |
| Eyes | | | | | |
| Nose | | | | | |
| Buccal mucosa | | | | | |
| Hard palate | | | | | |
| Soft palate | | | | | |
| Upper gingiva | | | | | |
| Lower gingiva | | | | | |
| Tongue | | | | | |
| Floor of Mouth | | | | | |
| Labial Mucosa | | | | | |
| Posterior Pharynx | | | | | |
| Anogenital | | | | | |
| Total Mucosa | /120 | | | | |

**Fig 3.** Objective bullous pemphigoid disease area index

out of 30 (Fig 2). This subjective itch score will not be combined with the objective part of the BPDAI (Fig 3). Eventually, a quality-of-life tool for BP will be necessary as well. The BPDAI will be undergoing validation studies, similar to the partial validation done thus far with the PDAI.[3]

## DISCUSSION AND CONCLUSION

Despite many trials evaluating therapeutic options for BP, it has been difficult to compare the results from these trials because of the large number of end points and definitions of disease. The formation of an international committee of bullous

disease experts able to meet face to face on a regular basis has provided a mechanism for developing agreement on these issues for BP. This statement with agreed-upon common definitions, and the ongoing discussion and refinement of proposed common measurements for patients with BP, are the initial and necessary steps toward progress in the clinical evaluation and therapy of BP. Further progress and advancement will require a continued unified effort.

The following individuals who were unable to attend the meetings contributed by e-mail to the discussions: Cheyda Chams-Davatchi, Karen Harman, Pilar Iranzo, and Gudula Kirtschig. Molly Stuart and Will Zmchik at the International Pemphigus and Pemphigoid Foundation assisted with meeting setup.

**REFERENCES**

1. Kirtschig G, Middleton P, Bennett C, Murrell DF, Wojnarowska F, Khumalo NP. Interventions for bullous pemphigoid. Cochrane Database Syst Rev 2010;10:CD002292.
2. Murrell DF, Dick S, Ahmed AR, Amagai M, Barnadas MA, Borradori L, et al. Consensus statement on definitions of disease, end points, and therapeutic response for pemphigus. J Am Acad Dermatol 2008;58:1043-6.
3. Rosenbach M, Murrell DF, Bystryn JC, Dulay S, Dick S, Fakharzadeh S, et al. Reliability and convergent validity of two outcome instruments for pemphigus. J Invest Dermatol 2009;129:2404-10.
4. Pfutze M, Niedermeier A, Hertl M, Eming R. Introducing a novel Autoimmune Bullous Skin Disorder Intensity Score (ABSIS) in pemphigus. Eur J Dermatol 2007;17:4-11.
5. Fiorentino DF, Garcia MS, Rehmus W, Kimball AB. A pilot study of etanercept treatment for pemphigus vulgaris. Arch Dermatol 2011;147:117-8.
6. Fivenson DP, Breneman DL, Rosen GB, Hersh CS, Cardone S, Mutasim D. Nicotinamide and tetracycline therapy of bullous pemphigoid. Arch Dermatol 1994;130:753-8.
7. Morel P, Guillaume JC. Treatment of bullous pemphigoid with prednisolone only: 0.75 mg/kg/day versus 1.25 mg/kg/day; a multicenter randomized study. Ann Dermatol Venereol 1984; 111:925-8.
8. Joly P, Roujeau JC, Benichou J, Picard C, Dreno B, Delaporte E, et al. A comparison of oral and topical corticosteroids in patients with bullous pemphigoid. N Engl J Med 2002;346:321-7.
9. Joly P, Roujeau JC, Benichou J, Delaporte E, D'Incan M, Dreno B, et al. A comparison of two regimens of topical corticosteroids in the treatment of patients with bullous pemphigoid: a multicenter randomized study. J Invest Dermatol 2009;129:1681-7.
10. Bernard P, Vaillant L, Labeille B, Bedane C, Arbeille B, Denoeux JP, et al. Incidence and distribution of subepidermal autoimmune bullous skin diseases in three French regions; Bullous Diseases French Study Group. Arch Dermatol 1995; 131:48-52.

BJD
British Journal of Dermatology

## Childhood subepidermal blistering disease with autoantibodies to type VII collagen and laminin-332

DOI: 10.1111/j.1365-2133.2010.10065.x

MADAM, Autoimmune subepidermal blistering diseases include bullous pemphigoid, pemphigoid gestationis, linear IgA bullous dermatosis, mucous membrane pemphigoid (MMP), anti-p200 pemphigoid, epidermolysis bullosa acquisita (EBA) and bullous systemic lupus erythematosus.[1] Patients with EBA have IgG autoantibodies to type VII collagen while some patients with MMP have autoantibodies to laminin-332.[2,3] We describe a juvenile case of subepidermal blistering disease with autoantibodies to both type VII collagen and laminin-332. The present case is unique because of its childhood onset and successful remission following only topical steroid therapy.

A 12-year-old Japanese girl presented with pruritic eruptions on her scalp. A few weeks later, widespread pruritic vesicles gradually developed over her whole body. The vesicles were seen both on erythematous and normal skin (Fig. 1a, b). Blisters and erosions also appeared in her oral mucosa, but there was no involvement of genital or ocular mucous membranes (Fig. 1c). Neither nail changes nor alopecia were observed. She had no family history of any blistering disorders or autoimmune disease. There was no preceding illness or history of medication/vaccination that might have triggered her disease.

General laboratory examinations revealed no apparent abnormalities except for an increased serum IgE level (668·8 IU $mL^{-1}$; normal < 100 for age 7–14 years). A skin biopsy was taken from the edge of one blister on her right forearm. Light microscopy showed a subepidermal blister with an inflammatory cell infiltrate consisting of mainly neutrophils in the upper dermis (Fig. 2a). Direct immunofluorescence of the patient's lesional skin showed *in vivo* linear deposits of IgG and C3 at the epidermal basement membrane zone (Fig. 2b). On the blistered area, deposition of IgG and C3 was demonstrated on the dermal side of the separated skin (arrows, Fig. 2b). Indirect immunofluorescence with the patient's serum on 1 mol $L^{-1}$ NaCl-split normal human skin showed IgG antibodies bound to the dermal side of the blister (Fig. 2c). Immunoblot analysis revealed that the patient's serum reacted with a 290-kDa protein in dermal extracts, and further with purified laminin-332 α3 protein (145, 165 kDa) (Fig. 2d, e). Laminin-332 was obtained from human keratinocytes and was purified using an antilaminin-332 affinity column as

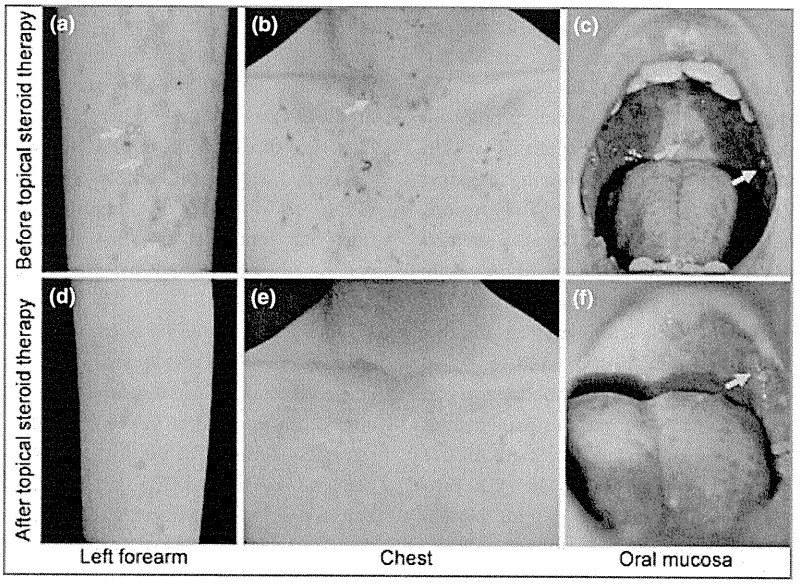


Fig 1. Clinical manifestations of the skin and oral mucosa. (a–c) Before topical steroid therapy. Erythema and tense vesicles on the left forearm and chest (a and b, arrows). Blisters and erosions over the oral mucosa (c, arrows). (d–f) After topical steroid therapy. Skin lesions healed within 9 days of the beginning of treatment, leaving residual pigmentation, scars and milia (d and e). Blisters and erosions on the oral mucosa subsided (f, arrow).

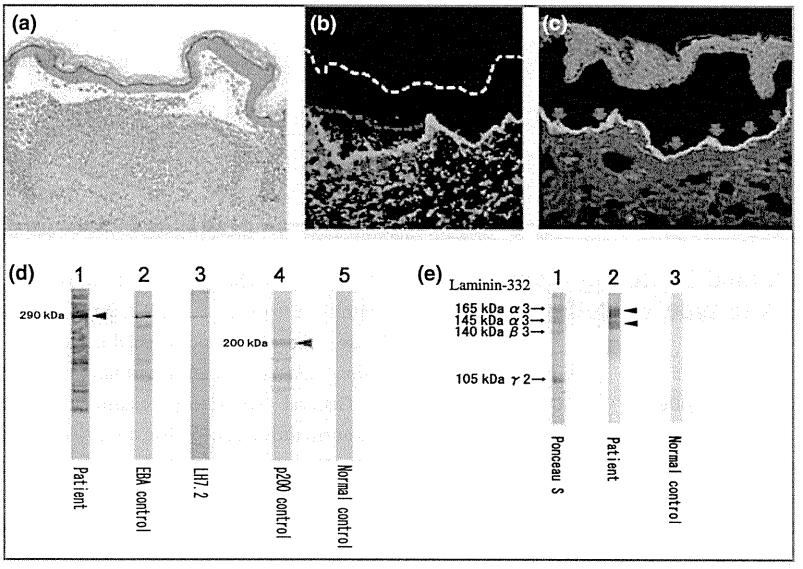


Fig 2. Histopathological findings, immunofluorescence staining and immunoblot analyses. (a) A subepidermal blister with an inflammatory cell infiltrate composed of mainly neutrophils in the upper dermis (haematoxylin and eosin; original magnification × 40). (b) Direct immunofluorescence showed *in vivo* linear deposits of IgG along the basement membrane zone. On the blister area, deposition of IgG was shown to be towards the dermal side of separated skin (arrows) (original magnification × 40; white dotted line is the skin surface and red dotted line is the roof side of separated skin). (c) Indirect immunofluorescence with the patient's serum on 1 mol $L^{-1}$ NaCl-split normal human skin showed IgG antibodies bound to the dermal side (arrows) (original magnification × 40). (d) Immunoblot analysis revealed that the patient's serum (lane 1), like both serum from a reference patient with epidermolysis bullosa acquisita (EBA, lane 2) and monoclonal antibody LH7.2 to type VII collagen (lane 3), reacted with a 290-kDa protein in dermal extracts (arrowhead). Control anti-p200 serum did not react with the 290-kDa but with a 200-kDa protein (red arrowhead) (lane 4). Normal control serum (lane 5) showed reactivity with neither. (e) In immunoblotting of purified laminin-332, lane 1 shows Ponceau S stain (protein staining using amido black). Reactivity with 145-kDa and 165-kDa purified laminin-332 α3 protein (arrowheads) was indicated in the patient's serum (lane 2), but not in the normal control serum (lane 3).

previously described.[4,5] Purified laminin-332 was a generous gift from Dr S. Amano, Shiseido Life Science Research Centre, Yokohama, Japan. The patient was diagnosed as having an autoimmune subepidermal blistering disease with circulating autoantibodies to type VII collagen and laminin-332.

Treatment was initiated with 0·05% clobetasol propionate ointment 20 g daily to skin lesions, which healed within 9 days after the beginning of treatment, leaving residual pigmentation, scars and milia (Fig. 1d, e). Blisters and erosions on the oral mucosa subsided without any topical therapy (Fig. 1f). The dose of topical corticosteroids was progressively decreased, and no recurrence of skin lesions was observed. The titre of antibasement membrane zone antibodies in indirect immunofluorescence studies decreased from 1 : 320 to 1 : 40 over 2 months. We performed further immunoblot analyses on five serial serum samples obtained from the patient after her antibasement membrane zone antibodies decreased. All five samples showed similar reaction bands to both 290-kDa protein in dermal extracts and purified laminin-332 α3 protein (145, 165 kDa) (data not shown). Hence it is difficult to speculate the major target antigen in this patient from these results. No local or systemic side-effects of topical corticosteroids were noticed during the entire treatment duration.

EBA and MMP are distinct autoimmune bullous diseases that are both characterized by autoantibodies to dermoepidermal junction components.[1] Detection of autoantibodies to either type VII collagen or laminin-332 differentiates these two diseases.[1] Interestingly, besides antitype VII collagen antibodies, circulating antilaminin-332 α3 antibodies were also found in our patient's serum. According to our survey of the literature, three other previous cases of subepidermal blistering disease with circulating antibodies to both type VII collagen and antilaminin-332 have been reported (Table 1).[6–8] All of the reported cases are of adult onset, thus our report is the first juvenile case. Similar to our patient, these reported patients all presented with mucosal involvement.

Our case is unique in its course and prognosis as well as age at onset. All of the previously reported patients needed systemic corticosteroids or immunosuppressant agents for proper disease control. In the studies by Jonkman *et al.*[6] and Umemoto *et al.*,[7] the bullous lesions of the patients relapsed after systemic prednisolone was tapered. The skin lesions of the patient reported by Baican *et al.*[8] were refractory to systemic prednisolone, azathioprine and dapsone. However, our juvenile case was successfully treated with only topical steroids, and no recurrence was observed in the following 6 months. Our case suggests that the treatment outcome and prognosis of juvenile cases are better than those of adult-onset cases. Further accumulation of similar juvenile cases is needed to confirm this hypothesis. The differ-

Table 1 Comparison of four reported patients with circulating antitype VII collagen and antilaminin-332 antibodies

| Patient | Age (years)/sex | Skin lesion | Mucosal involvement | Treatment | Outcome | Immunoblot analysis | Reference |
|---|---|---|---|---|---|---|---|
| 1 | 64/F | Blisters and erythema on the hands and feet | Oral/genital | Oral prednisolone 80 mg daily | Lesions resolved without scars/milia. Mild relapse occurred when tapering to oral prednisolone 5 mg daily | Type VII collagen, laminin-332 α3 | Jonkman *et al.*[6] |
| 2 | 46/M | Erythematous plaque, blisters, erosions and crusts on the trunk and extensor aspects of extremities | Oral | Oral colchicine 1·5 mg daily (refractory to prednisolone, azathioprine and dapsone) | Previous lesions healed with milia and scars. Free of new blisters but erythematous plaque persisted with erosions and crusts | Type VII collagen, laminin-332 α3, γ2 | Baican *et al.*[8] |
| 3 | 35/F | Vesicular lesions on the face, neck and upper back | Oral/genital | Oral prednisolone 40 mg daily | Lesions resolved without scars/milia. Mild relapse occurred when tapering to oral prednisolone 25 mg daily | Type VII collagen, laminin-332 α3, β3 | Umemoto *et al.*[7] |
| 4 | 12/F | Blisters, erosions and erythema on the face, trunk, hands and feet | Oral | Topical clobetasol propionate ointment 20 g daily | Lesions resolved with scars and milia. No recurrence was found | Type VII collagen, laminin-332 α3 | Our patient |

ences between childhood-onset and adult-onset cases seem to mirror those of EBA at different ages. Compared with adult cases, childhood EBA cases respond relatively better to treatment, and usually low-dose oral prednisolone and dapsone are effective and sufficient.[1]

In conclusion, we report the first juvenile case with autoantibodies to both type VII collagen and laminin-332, successfully treated with only topical steroid therapy. Our case suggests that juvenile cases have different characteristics from those of adult-onset cases in their course, including treatment outcome and prognosis. As topical steroid therapy has several advantages over systemic corticosteroids due to less severe complications, we consider topical steroids as preferable to systemic steroids for childhood-onset autoimmune subepidermal bullous disease.

*Department of Dermatology, Hokkaido University Graduate School of Medicine, Sapporo, Japan*
*Correspondence: Teruki Yanagi.*
*E-mail: yanagi@med.hokudai.ac.jp*

H.-Y. Lin
T. Yanagi
M. Akiyama
M.M. Iitani
R. Moriuchi
K. Natsuga
S. Shinkuma
N. Yamane
D. Inokuma
K. Arita
H. Shimizu

## References

1 Fine JD. Management of acquired bullous skin diseases. *N Engl J Med* 1995; **333**:1475–84.
2 Mayuzumi M, Akiyama M, Nishie W *et al.* Childhood epidermolysis bullosa acquisita with autoantibodies against the noncollagenous 1 and 2 domains of type VII collagen: case report and review of the literature. *Br J Dermatol* 2006; **155**:1048–52.
3 Domloge-Hultsch N, Anhalt GJ, Gammon WR *et al.* Anti-epiligrin cicatricial pemphigoid: a subepithelial bullous disorder. *Arch Dermatol* 1994; **130**:1521–9.
4 Natsuga K, Nishie W, Shinkuma S *et al.* Circulating IgA and IgE autoantibodies in antilaminin-332 mucous membrane pemphigoid. *Br J Dermatol* 2010; **162**:513–17.
5 Amano S, Nishiyama T, Burgeson RE. A specific and sensitive ELISA for laminin 5. *J Immunol Methods* 1999; **224**:161–9.
6 Jonkman MF, Schuur J, Dijk F *et al.* Inflammatory variant of epidermolysis bullosa acquisita with IgG autoantibodies against type VII collagen and laminin alpha3. *Arch Dermatol* 2000; **136**:227–31.
7 Umemoto N, Demitsu T, Toda S *et al.* A case of nonscarring subepidermal blistering disease associated with autoantibodies reactive with both type VII collagen and laminin 5. *Dermatology* 2003; **207**:61–4.
8 Baican A, Hirako Y, Lazarova Z *et al.* IgG antibodies to type VII collagen and an exclusive IgG3 reactivity to the laminin alpha3 chain in a patient with an autoimmune subepidermal blistering disease. *J Am Acad Dermatol* 2005; **53**:517–22.

Funding sources: none.

Conflicts of interest: none declared.

**Disease Models & Mechanisms** 4, 777-785 (2011) doi:10.1242/dmm.007146

**RESEARCH ARTICLE**

# Abca12-mediated lipid transport and Snap29-dependent trafficking of lamellar granules are crucial for epidermal morphogenesis in a zebrafish model of ichthyosis

Qiaoli Li[1,*], Michael Frank[1,*], Masashi Akiyama[2,3], Hiroshi Shimizu[3], Shiu-Ying Ho[4], Christine Thisse[5], Bernard Thisse[5], Eli Sprecher[6] and Jouni Uitto[1,4,‡]

## SUMMARY

Zebrafish (*Danio rerio*) can serve as a model system to study heritable skin diseases. The skin is rapidly developed during the first 5-6 days of embryonic growth, accompanied by expression of skin-specific genes. Transmission electron microscopy (TEM) of wild-type zebrafish at day 5 reveals a two-cell-layer epidermis separated from the underlying collagenous stroma by a basement membrane with fully developed hemidesmosomes. Scanning electron microscopy (SEM) reveals an ordered surface contour of keratinocytes with discrete microridges. To gain insight into epidermal morphogenesis, we have employed morpholino-mediated knockdown of the *abca12* and *snap29* genes, which are crucial for secretion of lipids and intracellular trafficking of lamellar granules, respectively. Morpholinos, when placed on exon-intron junctions, were >90% effective in preventing the corresponding gene expression when injected into one- to four-cell-stage embryos. By day 3, TEM of *abca12* morphants showed accumulation of lipid-containing electron-dense lamellar granules, whereas *snap29* morphants showed the presence of apparently empty vesicles in the epidermis. Evaluation of epidermal morphogenesis by SEM revealed similar perturbations in both cases in the microridge architecture and the development of spicule-like protrusions on the surface of keratinocytes. These morphological findings are akin to epidermal changes in harlequin ichthyosis and CEDNIK syndrome, autosomal recessive keratinization disorders due to mutations in the *ABCA12* and *SNAP29* genes, respectively. The results indicate that interference of independent pathways involving lipid transport in the epidermis can result in phenotypically similar perturbations in epidermal morphogenesis, and that these fish mutants can serve as a model to study the pathomechanisms of these keratinization disorders.



## INTRODUCTION

### Clinical and genetic heterogeneity of ichthyosis

Ichthyosis comprises a group of both acquired and heritable keratinization disorders characterized by hyperkeratotic and scaly skin (Brown and Irvine, 2008). Although the phenotypic spectrum of ichthyosiform dermatoses is extremely broad, with either limited or extensive involvement of the skin, among the inherited forms, three clinically and genetically distinct subtypes have been identified: ichthyosis vulgaris, X-linked ichthyosis and lamellar ichthyosis (LI) (McGrath and Uitto, 2008; Brown and Irvine, 2008; Brown and McLean, 2008; Elias et al., 2004). LI in itself is a heterogeneous group of autosomal recessive disorders with large plaque-like brown scales over most of the body, associated with ectropion and alopecia.

Harlequin ichthyosis (HI) is a rare, extremely severe form of ichthyosis, most closely associated with the LI group of these disorders (Akiyama, 2006a). Neonates are born encased in a thick skin that not only restricts their movement, but also distorts their facial features, averting their lips and eyelids. Although newborns with HI frequently die within the first few days of life, a few of these affected individuals do survive, and their skin eventually resembles severe non-bullous congenital ichthyosiform erythroderma or LI.

HI is an autosomal recessive disorder caused by mutations in the ATP-binding cassette, sub-family A, member 12 (*ABCA12*) gene, which encodes a lipid transporter protein localized to lamellar granules in epidermal keratinocytes (Sakai et al., 2007). Mutations in the *ABCA12* gene result in congested lipid secretion and impaired barrier function of the stratum corneum (Kelsell et al., 2005). Thus, *ABCA12* is crucial to the development of the skin-lipid barrier in the stratum corneum.

An *Abca12*$^{-/-}$ mouse model has been vital in confirming the role of this transporter molecule in the skin abnormalities seen in HI, i.e. hyperkeratosis, impaired barrier function, abnormal lamellar bodies and the retention of lipid droplets in the epidermis (Yanagi et al., 2008; Smyth et al., 2008; Sundberg et al., 1997). The role of Abca12 in transporting lipids was confirmed by culturing keratinocytes from *Abca12*$^{-/-}$ mice and observing impaired lipid

[1]Department of Dermatology and Cutaneous Biology, and [4]Department of Biochemistry and Molecular Biology, Jefferson Medical College, Thomas Jefferson University, Philadelphia, PA 19107, USA
[2]Department of Dermatology, Nagoya University Graduate School of Medicine, Nagoya 466-8550, Japan
[3]Department of Dermatology, Hokkaido University Graduate School of Medicine, Sapporo 060-8638, Japan
[5]Department of Cell Biology, University of Virginia School of Medicine, Charlottesville, VA 22908, USA
[6]Department of Dermatology, Tel Aviv Medical Center, Tel Aviv 64239, Israel
*These authors equally contributed to this work
‡Author for correspondence (Jouni.uitto@jefferson.edu)

Received 29 October 2010; Accepted 27 May 2011

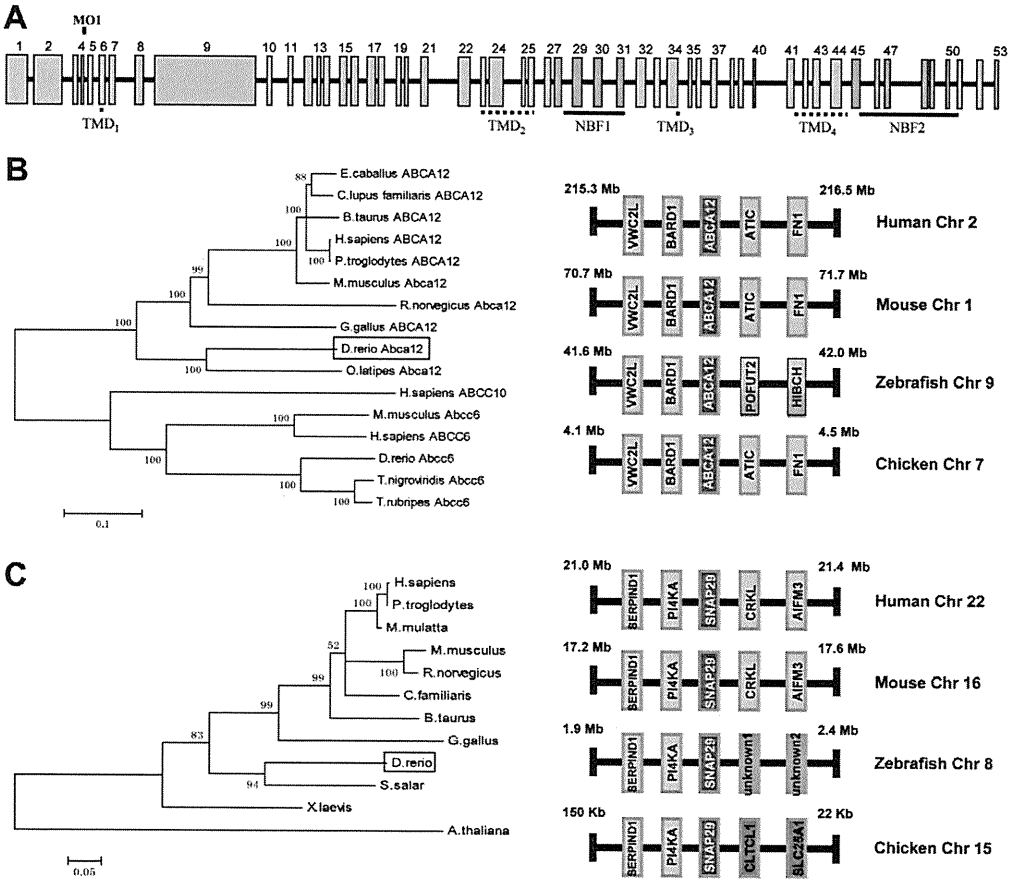


**Fig. 1. Schematic representation of the zebrafish *abca12* gene, and the phylogenetic trees of the protein sequences of Abca12 and Snap29, together with syntenic analysis of the corresponding genes.** (A) The *abca12* gene consists of 53 exons, which are numbered on the top, and the coding segments for transmembrane domains (TMDs) and nucleotide binding folds (NBFs; green) are underlined. Note the location corresponding to the morpholino (MO1) at the exon-4–intron-4 junction. (B) The phylogenetic relationship between zebrafish Abca12 and the other members of the ABC family of transporters estimated by the neighbor-joining method (left panel). The syntenic analysis of the *abca12* and flanking genes in human, mouse, zebrafish and chicken chromosomes is shown on right. (C) Cladogram and syntenic analysis of *snap29*. The unknown genes 1 and 2 in zebrafish chromosome 8 have been designated as si:dkey-178e17.1 and si:dkeyp-117b11.1, respectively.

efflux leading to intracellular accumulation of lipids, specifically ceramides (Akiyama et al., 2005). However, the drawback of the mouse model is the long gestation period and small number of offspring per litter.

In addition to nonsyndromic variants, ichthyosis can be associated with clinical manifestations in a number of organ systems besides the skin. An example of syndromic ichthyoses is the CEDNIK syndrome, a rare autosomal recessive disorder with cerebral dysgenesis, neuropathy, ichthyosis and keratoderma. This syndrome has been shown to be associated with mutations in the *SNAP29* gene, which encodes soluble n-ethylmaleimide sensitive factor (NSF) attachment protein (SNAP)29, a member of the SNAP receptor (SNARE) family of proteins (Sprecher et al., 2005; Fuchs-Telem et al., 2011). SNARE proteins are required for vesicle trafficking and they mediate the fusion between the vesicles and their target membranes. *SNAP29* deficiency has been suggested to result in impaired maturation and secretion of lamellar granules, particularly interfering with the transport of lipids to stratum corneum; however, no animal model for the CEDNIK syndrome exists.

In an attempt to create an alternative, and perhaps more expedient, model system to study ichthyosis, we have performed work on zebrafish (*Danio rerio*), which has nearly the same complement of genes as mammals. Some of the benefits to working with zebrafish include their rapid development and the ease with which one can manipulate their gene expression by morpholino-based antisense oligonucleotides (Kari et al., 2007; Li et al., 2011). Zebrafish develop rapidly, with all major organs, including the skin, having developed by 5-6 days post-fertilization (dpf). They also produce a large number of embryos per laying, approximately 50-100 per female. In this study, we performed experiments to show that *abca12* and *snap29* gene knockdown in zebrafish causes epidermal changes that are similar, attesting to the concept that diverse pathogenetic pathways, as a result of mutations in different genes, can result in phenotypes in the spectrum of ichthyotic diseases. Thus, zebrafish provide a novel and expedient model system to study this group of devastating, currently intractable, diseases.

## RESULTS

### Identification of an *ABCA12*-related gene in the zebrafish genome

Search of the online gene database (NCBI) identified one human *ABCA12*-related sequence, *abca12*, which mapped to zebrafish chromosome 9. This zebrafish *abca12* gene had an open reading frame, and all splice sites appeared intact, which allowed deduction of the intron-exon organization. The *abca12* gene consists of 53 exons, with sizes ranging from 55 to 2415 bp (Fig. 1A). The predicted primary sequence of the corresponding protein consists of 3634 amino acids, whereas the corresponding human primary sequence comprises 2595 amino acids. The overall conservation at the protein level was 49.3% and, consequently, the zebrafish *abca12* gene can be considered to be the human *ABCA12* homolog.

Alignment of human and zebrafish protein sequences revealed that zebrafish Abca12 has an extended 486 amino acid N-terminal sequence, as well as a number of insertions in the N-terminal half of the protein. However, alignment of zebrafish and human sequences identified conservation of domains that are characteristic of the ABC transporter proteins. Specifically, the zebrafish sequence, similar to the human sequence, was predicted to consist of four transmembrane domains (TMD1-4) and to contain two nucleotide binding fold domains (NBF1 and NBF2) (Tusnády et al., 2006) (Fig. 1A). The NBFs displayed characteristic sequences for Walker A and B motifs, as well as a highly conserved ABC signature sequence. Comparison of the deduced amino acid sequence within the NBF1 domain of zebrafish Abca12 showed 74% identity to the corresponding NBF1 domain in the human protein, whereas the NBF2 domain had 68% identity to human NBF2.

### Evolutionary conservation of zebrafish *abca12*

Differences between the zebrafish *abca12* gene and homologous genes in other species were examined by phylogenetic analysis of the corresponding protein sequence by cladistic measurement (Fig. 1B). The cladogram suggested that the zebrafish gene is distant from most of the other *ABCA12*-related genes in a number of species, and, therefore, presumably diverged early. However, inclusion of other members of the ABC transporter family, such as ABCC10 and ABCC6, in different species, serving as an outgroup, indicated that the zebrafish Abca12 protein sequence is closer to human ABCA12 than it is to the sequences in the outgroup. To confirm that the zebrafish *abca12* is the correct ortholog of human *ABCA12*, syntenic analysis of *Abca12* in different species was performed (Fig. 1B). These analyses revealed that *ABCA12* and its flanking genes, *VWC2L* and *BARD1*, were located on the same chromosome in the same gene order in human, mouse, zebrafish and chicken genomes (Fig. 1B).

### Expression of the zebrafish *abca12* gene during early embryonic development

The temporal expression profile of *abca12* was examined in embryos collected during the first 8 days of development, and the corresponding mRNA levels were determined by reverse transcriptase (RT)-PCR. An undetectable level of expression was noted in embryos at the time of fertilization [0 hours post-fertilization (hpf)], but detectable levels of mRNA transcripts were noted at 6 hpf, with a significant further increase by 1 dpf. During the subsequent days (2-8 dpf), the expression levels remained relatively constant in comparison with the control gene, *β-actin* (Fig. 2A).

### Whole-mount in situ hybridization of *abca12* in zebrafish

To determine the spatial expression of *abca12* during different stages of zebrafish development, whole-mount in situ hybridization was performed using probes specific for the *abca12* gene (Fig. 2B). An antisense probe for *abca12* gave specific expression patterns. During the gastrula period, expression of *abca12* was observed in cells of the enveloping layer (EVL; Fig. 2B). Expression of the *abca12* gene in this tissue, which is named periderm after the end of gastrulation, is observed until the end of embryonic development. After 24 hpf, expression of *abca12* was also observed, although at lower levels, in the olfactory vesicle as well as in mucus-secreting cells (Fig. 2B). At the end of embryonic development, expression was observed mainly in olfactory vesicle, pharynx and mucus-secreting cells. A sense probe was used as a control and did not give a specific expression pattern.

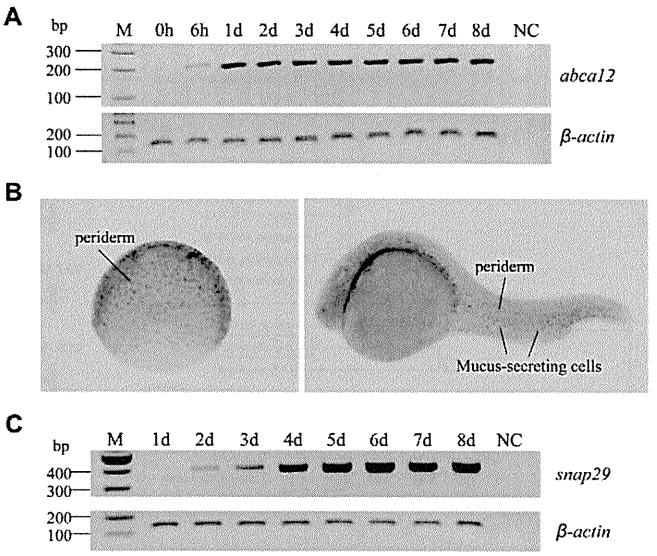


**Fig. 2. *abca12* and *snap29* gene expression in normal zebrafish.** (A-C) Zebrafish embryos were collected at 0 and 6 hpf and 1-8 dpf, and total RNA was isolated and cDNA prepared. The *abca12* (A) and *snap29* (C) mRNA expression levels were measured by RT-PCR and standardized against the mRNA expression level of the *β-actin* gene. (B) Whole-mount in situ hybridization of embryos at different stages of early development for *abca12* expression; gastrula period (left panel), 24 hpf (right panel).

### Morpholino knockdown of *abca12* expression results in an altered skin phenotype

Morpholino antisense oligonucleotide (MO1) directed against a splice donor site in *abca12* was injected into one- to four-cell-stage embryos, and amplification of total RNA was performed by primers corresponding to exons 4 and 5. Using these primers, PCR amplification of *abca12* cDNA resulted in a 189 bp product, whereas amplification of genomic DNA generated a 356 bp product (Fig. 3A). RT-PCR of total RNA extracted from zebrafish 3 days after injection with MO1 revealed that essentially all (>90%) of the pre-mRNA remained unprocessed, attesting to the efficiency of the morpholino knockdown (Fig. 3A). Injection of control morpholinos, either a global standard control MO (scMO) or 5-bp mismatched control (cMO), had no effect on pre-mRNA processing (Fig. 3A).

The effect of the injection of morpholinos into one- to four-cell embryos was first examined by determining the survival of the embryos. Of the 180 embryos injected with *abca12* MO1, 76% survived at 3 dpf, a number that did not statistically differ from the survival of embryos injected with standard control morpholino (81%) (Table 1). At 5 dpf, the survival of embryos injected with MO1 was only 6%, a statistically significant reduction from the survival noted with scMO and uninjected controls (81% and 87%, respectively; $P<0.0001$) (Table 1).

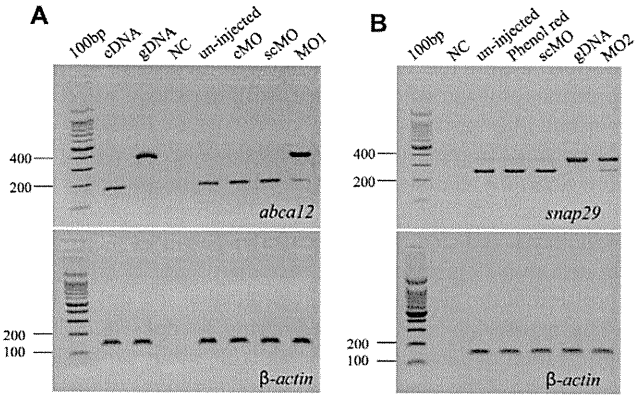


**Fig. 3. Knockdown of *abca12* and *snap29* expression by morpholinos.** (A) Knockdown of *abca12*. (B) Knockdown of *snap29*. MO1 and MO2 morpholinos (right lanes, the upper panel), which target the splice donor site at the exon-4–intron-4 border of the corresponding genes, prevents pre-mRNA splicing. The consequences of MO1 on *abca12* pre-mRNA splicing and MO2 on *snap29* mRNA splicing were determined by RT-PCR. The results showed the retention of intron 4 in the majority of mRNA transcripts (>90%) as compared with the normally transcribed control. The mRNA levels were normalized by the level of *β-actin* mRNA (lower panels). cDNA and gDNA represent amplification of the corresponding complementary DNA and genomic DNA, respectively. Injections with the 5-bp mismatched control morpholino for *abca12* (cMO) or global standard control morpholino (scMO) did not alter pre-mRNA processing, similar to the uninjected controls or those injected with phenol red.

Examination of the morphology of zebrafish larvae injected with MO1 ($n$=180) revealed profound changes during development. Although no differences were noted between the morphant and control larvae at 1 dpf, by 3 dpf the morphants had developed noticeable changes in the distribution of pigment along their trunk and tail, in addition to pericardial edema (Fig. 4A). Upon careful examination at 3 dpf, 92% of larvae displayed yolk sac enlargement and severe disruption of their chromatophore distribution, with 75% exhibiting concomitant pericardial edema (Table 1).

### Altered epidermal morphology in the morphant larvae

To examine the consequences of the morpholino-mediated knockdown of *abca12* expression in the skin of zebrafish, we first used scanning electron microscopy (SEM) to examine the surface contour and cellular morphology of the epidermis. In 3-dpf controls ($n$=21), well-demarcated keratinocytes with distinct borders and characteristic microridges were observed (Fig. 5). Examination of the skin surface of the morphant larvae ($n$=4) revealed perturbations in the architecture of the microridges, with spicules protruding from the center of each keratinocyte. Thus, the development of the top layer of skin during the first 3 days of zebrafish development was perturbed in the absence of Abca12 activity.

Alterations in the epidermis at 3 dpf were further examined by transmission electron microscopy (TEM) both in control and morphant larvae ($n$=4 in each group). At this developmental stage, normal epidermis consists of two unicellular layers, the superficial layer and the basal layer. The contour of the outer surface of the superficial layer is studded with spicules that correspond to the microridges noted previously on SEM (Fig. 6A). The epidermis rests on a basement membrane, which separates the epidermis from the underlying developing dermis.

The epidermis of the morphant larvae similarly consisted of two cell layers resting on a basement membrane (Fig. 6B). However, in contrast to the control larvae, both layers of the morphant epidermis contained an abundance of electron-dense granules, approximately 440 nm in average diameter. Closer examination of these aggregates at higher magnification suggested the presence of lipid-like vesicles within the larger electron-dense granules (Fig. 6C,D). It should be noted that, although somewhat similar aggregates of electron-dense material were noted in the epidermis of the control specimens, they were localized only to the area of the superficial layer just below the microridges.

### Co-injection of human *ABCA12* mRNA rescues the morpholino-mediated phenotype

To test the specificity of the phenotypic changes associated with MO1 injection, a rescue experiment with co-injection of in vitro transcribed human *ABCA12* mRNA was performed. The injection of MO1 alone caused characteristic phenotypic changes, whereas co-injection of human mRNA together with MO1 partially rescued the phenotype (Fig. 4A,B). Specifically, at 5 dpf, the survival of the co-injected larvae was 62%, which is statistically different from the 6% in those injected with MO1 alone ($P$<0.0001) (Table 1). Also, 27% of co-injected larvae ($n$=184) had a phenotype that was indistinguishable from the controls. In the remaining 73% of co-injected larvae, the degree of yolk sac enlargement and chromatophore disorganization was noticeably less than in the larvae injected with MO1 alone. Of this 73%, 70% also manifested

**Table 1. Survival of and development of phenotype in zebrafish injected with *abca12* morpholino**

| Experimental group | No. of fish | 3 dpf | | | 5 dpf | | |
|---|---|---|---|---|---|---|---|
| | | Survival (%) | Skin phenotype (%) | Edema (%) | Survival (%) | Skin phenotype (%) | Edema (%) |
| Uninjected control | 152 | 87 | 0 | 0 | 87 | 0 | 0 |
| scMO | 177 | 81 | 0 | 0 | 81 | 0 | 0 |
| *abca12* MO1 | 180 | 76 | 92[a] | 75[a] | 6[a] | 0 | 0 |
| *abca12* MO1+ hABCA12 mRNA | 184 | 87[b] | 81[b] (milder) | 74 (milder) | 62[c] | 73[c] (milder) | 70[c] (milder) |

This is a representative experiment in which all groups were followed in parallel. Similar results were obtained in >ten additional experiments with the same design. Skin phenotype refers to epidermal perturbations, disruption of the chromatophore distribution and yolk sac enlargement. Edema is pericardial edema.
scMO, standard control morpholino with no biological function and no target sequence in zebrafish genome (Robu et al., 2007).
[a]Statistical significance between the *abca12* MO1 group and scMO group (Fisher's exact test: $P$<0.0001).
[b,c]Statistical significance between the *abca12* MO1 group and the *abca12* MO1+hABCA12 mRNA group (Fisher's exact test: [b]$P$<0.05; [c]$P$<0.0001).

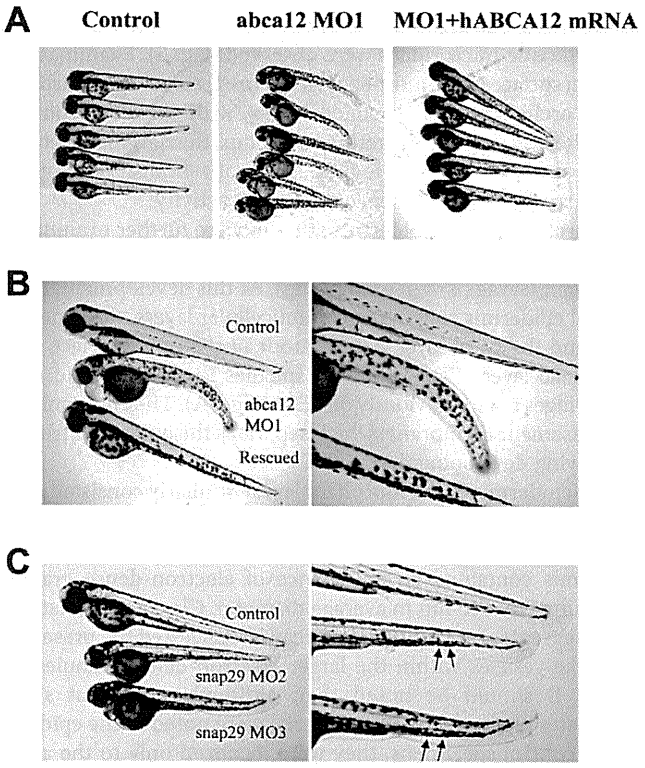


**Fig. 4. Zebrafish phenotypes and their mRNA rescue at 3 dpf.**
(A) Phenotypic appearance of zebrafish larvae after injection with an *abca12* MO1 morpholino (middle panel) compared with control larvae (left panel), and partial rescue with human *ABCA12* mRNA (right panel). (B) Higher magnification of the larvae shown in A. (C) Phenotype of larvae at 3 dpf injected with *snap29* morpholinos MO2 or MO3. The irregular contour of the epidermis is noted by arrows.

pericardial edema. The rescue experiment, in addition to injection of control morpholinos, attested to the specificity of the phenotype documented in the morphant larvae. These experiments also confirmed that the zebrafish *abca12* gene is the functional homolog of human *ABCA12*.

### Epidermal perturbations in zebrafish injected with *snap29* morpholino

Because knockdown of *abca12* expression was speculated to interfere with lipid secretion by lamellar granules, resulting in a characteristic epidermal phenotype, we proceeded to test this postulate by interfering with the lipid transport by another, independent mechanism: knockdown of the expression of the *snap29* gene. The corresponding protein, Snap29, has been suggested to mediate lipid transport within the epidermis and the deficiency of SNAP29 expression results in syndromic ichthyosis in patients with CEDNIK syndrome (Rapaport et al., 2010; Sprecher et al., 2005).

Surveying the zebrafish genome database revealed the presence of one *SNAP29*-related gene, *snap29*, on chromosome 8. This gene product had 52% identity with the human gene product at the protein level, and cladogram and syntenic analyses suggested that zebrafish *snap29* is the ortholog of human *SNAP29* (Fig. 1C). The expression of the gene was readily detectable at 2 dpf by RT-PCR and the expression level increased during 3-8 dpf (Fig. 2C). In situ hybridization of larvae showed weak, ubiquitous expression with accentuation of the labeling in the central nervous system marginal zone (not shown).

Injection of a morpholino (MO2) placed on the exon-4–intron-4 junction of the *snap29* gene into one- to four-cell-stage embryos inhibited the processing of pre-mRNA by >90% (Fig. 3B). A second, non-overlapping morpholino (MO3), placed on the intron-4–exon-5 border of the *snap29* gene similarly resulted in >90% inhibition of the splicing of intron 4 (data not shown). Examination of the morphant larvae at 3 dpf ($n$=165 for MO2, and $n$=203 for MO3) revealed a phenotype consisting of pigmentary changes, somewhat analogous with those noted with the *abca12* morpholino, in 80% of larvae, and the contour of the epidermis in the tail section was irregular (Fig. 4C). SEM of 20 morphant larvae revealed perturbations in the morphology of the epidermis that were very similar to those noted as a result of *abca12* knockdown (Fig. 5). Examination of the epidermis of the *snap29* morphant larvae ($n$=4) by TEM at 3 dpf revealed an increase in vesicles, which appeared empty under the same fixation conditions that revealed accumulation of lipid-like material in *abca12* morphant fish (Fig. 6E,F). Thus, interference by morpholino knockdown of the expression of two independent genes, *abca12* and *snap29*, that are involved in lipid transport in the epidermis can lead to similar phenotypic alterations in the epidermal morphology.

## DISCUSSION

### *ABCA12* mutations underlie HI

The molecular basis of HI is linked to mutations in the *ABCA12* gene (Akiyama et al., 2005; Kelsell et al., 2005). Initial approaches utilizing single-nucleotide polymorphism-based chip technology and homozygosity mapping of families with individuals affected with HI placed the candidate gene locus on chromosomal region 2q35, and microsatellite markers narrowed the interval to consist of six genes (Kelsell et al., 2005). Several previous observations pointed to *ABCA12* as a candidate gene within the critical region. First, a characteristic ultrastructural feature of the epidermis in HI is an abnormality in the

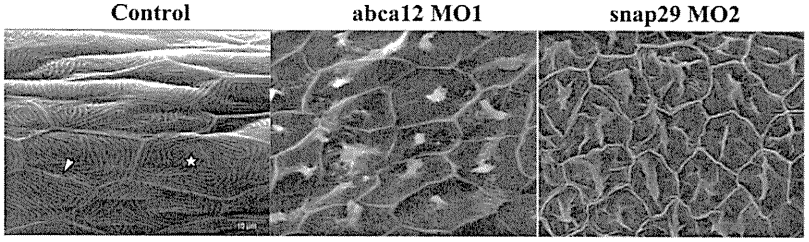


**Fig. 5. SEM of the skin surface.** The skin of the tail of the control larvae injected with the global standard control morpholino at 3 dpf shows the presence of keratinocytes with well-demarcated cell-cell borders (arrowhead) containing microridges (star; left panel). The morphant larvae injected with MO1 morpholino for *abca12* (middle) or *snap29* (MO2; right panel) revealed perturbed microridge formation with spicules in the center of the keratinocytes.

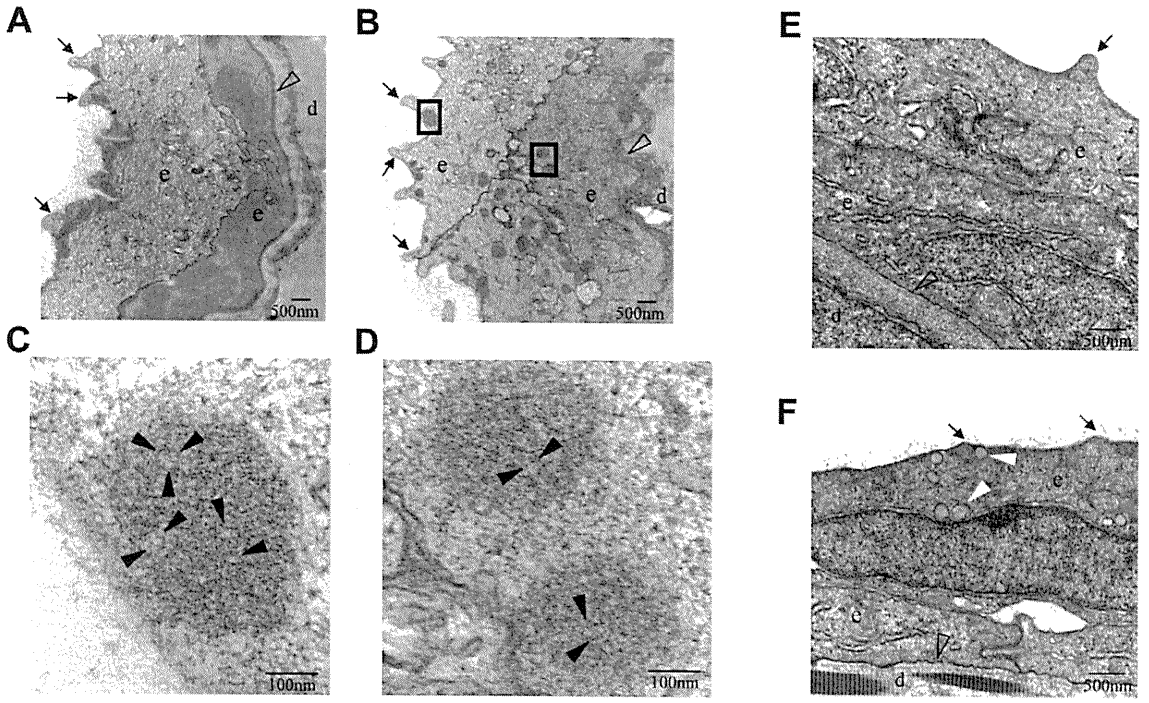


**Fig. 6. TEM of 3-dpf larvae injected with *abca12* or *snap29* morpholinos.** (A,E) Control morpholino (scMO); (B) *abca12* morpholino (MO1). Boxes surrounding electron-dense subcellular structures in B were examined at higher magnification and are shown in C and D. (F) Injection with *snap29* morpholino (MO2). (A-F) Arrows point to microridges; open arrowheads indicate basement membrane; solid black arrowheads point to the areas of accumulation of putative lipids within the electron-dense granules in C and D; solid white arrowheads in F point to apparently empty vesicles. e, epidermis; d, developing dermis.

localization of epidermal lipids, together with abnormal ultrastructural epidermal lamellar granules (Akiyama, 2006b). *ABCA12* has been suggested to encode a transmembrane transporter protein, which, from sequence homology with several other ABC family members, was thought to be involved in the transport of lipids (Kaminski et al., 2006). Second, the *ABCA12* gene was previously shown to harbor missense mutations in a milder form of ichthyosis, lamellar ichthyosis type 2 (LI2), with some resemblance to the phenotype in patients with HI who survive beyond the immediate postnatal period (Lefèvre et al., 2003). Currently, a total of 53 distinct mutations have been identified in the *ABCA12* gene (Akiyama, 2010).

Expression of *ABCA12* has been localized to lamellar granules. In normal epidermal keratinocytes there is an upregulation of *ABCA12* expression in association with physiological keratinization of the human epidermis (Sakai et al., 2007). Mutations in the *ABCA12* gene result in congested lipid retention in the skin of individuals with HI. It has been suggested that ABCA12 transports ceramides, the major lipid of the stratum corneum of the epidermis. Finally, lamellar-granule-mediated lipid secretion was resumed in the cultured keratinocytes of patients with HI upon transfer of the wild-type *ABCA12* gene (Akiyama et al., 2005). Thus, it is clear that mutations in the *ABCA12* transporter gene underlie HI.

### *abca12* and zebrafish skin development

In this study, we have demonstrated that zebrafish *abca12* is the ortholog of human *ABCA12*. There is a high degree of conservation of the Walker A and B motifs in addition to the retention of the four transmembrane domains containing one, five, one and five transmembrane segments, respectively. Zebrafish NBF1 and NBF2 domains in the Abca12 protein have 74% and 68% similarity with human NBF1 and NBF2 domains, respectively, at the amino acid level.

Whole-mount in situ hybridization in developing zebrafish embryos revealed that *abca12* was expressed in the EVL and the periderm. The EVL first appears at the 64-cell stage of development (~2 hpf) and is the outermost monolayer of cells surrounding the embryo. The EVL eventually gives rise to the periderm, which is thought to ultimately be replaced by the superficial stratum of the epidermis (Kimmel et al., 1995; Le Guellec et al., 2004). Although the physiology of zebrafish skin is still largely unexplored, the fact that *abca12* is expressed in the skin suggests its importance in normal skin development. This hypothesis is further strengthened by the results from our morpholino experiments. Injecting a morpholino that inhibited pre-mRNA splicing by >90% produced alterations in chromatophore distribution and the abnormal retention of lipids in both layers of the epidermis. Not only does this suggest that *abca12* is responsible for lipid transport in zebrafish, but the abnormal accumulation of lipids throughout the epidermis is a frequent finding in individuals with HI. Finally, the rescue of this phenotype by co-injection of human *ABCA12* mRNA shows that the phenotype is the result of *abca12* knockdown and not due to an off-target effect. In this context, it should be emphasized that the EVL-derived skin in zebrafish is embryologically different from the mammalian skin. Specifically, zebrafish epidermis does not undergo terminal differentiation, which in human skin culminates in the development of stratum corneum with barrier function. Emphasizing this

difference is the fact that survey of the current zebrafish genome database (Ensembl, Zebrafish Zv9; http://www.ensembl.org/Danio_rerio/Info/Index) does not reveal the presence of filaggrin, involucrin and trichohyalin genes, which are crucial for development of the stratum corneum in human epidermis (Li et al., 2011).

The role of lipids in epidermal development is further emphasized by our findings that knockdown of the expression of an independent gene, *snap29*, results in a similar epidermal phenotype as noted in *abca12* mutant larvae. Snap29 has been postulated to mediate lipid transport in the epidermis by facilitating membrane fusion of lamellar granules (Sprecher et al., 2005). Thus, interference of lipid trafficking by knockdown of two independent genes results in phenocopies of the epidermal perturbations in zebrafish, mimicking epidermal alterations in different forms of ichthyosis. It should be noted that, similar to the CEDNIK syndrome, ichthyosis has been reported in association with mental retardation, enteropathy, deafness, peripheral neuropathy and keratodermia, dubbed as the MEDNIK syndrome (Montpetit et al., 2008). This constellation was shown to be associated with a homozygous splice-site mutation in the *AP1S1* gene, encoding a subunit of the adaptor protein complex that regulates clathrin-coated vesicle assembly, protein cargo sorting, and vesicular trafficking between organelles in eukaryotic cells (Montpetit et al., 2008). The pathogenic effect of this mutation was validated by knockdown of *ap1s1* expression in zebrafish by a morpholino, resulting in perturbation in skin formation, reduced pigmentation and motility deficits. These findings, together with our observations in *snap29* mutant larvae, attest to the importance of vesicular trafficking in epidermal morphogenesis.

As indicated by morphological observations of the developing epidermis in zebrafish in comparison with human skin, there are clear differences. For example, the embryological origin of the EVL (periderm) in zebrafish is distinct from the basal layer in embryonic skin. In spite of this difference, there is an increasing body of evidence suggesting that the underlying molecular differentiation pathways are conserved between mammals and the zebrafish epidermis, based on molecular homologies (Sabel et al., 2009; Slanchev et al., 2009). Our work highlighting the early *abca12* expression in the EVL seems to support the conclusions that EVL forms the external layer of the embryonic and larval dermis and represents the initial differentiation of a true epidermis (Fukazawa et al., 2010).

Collectively, our results highlight the role of lipid transport and vesicular trafficking in epidermal development, and the results further suggest that zebrafish can serve as a model system to study different variants of ichthyosis, such as HI and the CEDNIK syndrome. Besides increasing our understanding of the disease mechanisms involved in ichthyotic syndromes, this model system is potentially useful for testing novel treatment modalities, for example by performing a small molecule library screen for compounds that are able to suppress the phenotype.

## METHODS

### Maintenance of zebrafish

Adult wild-type zebrafish were maintained under standard conditions at 28.5°C. Zebrafish embryos and larvae were also maintained at 28.5°C in a special embryo medium. All animals were housed in the zebrafish facility at Thomas Jefferson University and were cared for and used in accordance with University Institutional Animal Care and Use Committee guidelines and permission.

### Phylogenetic and syntenic analyses

The genomic sequences of zebrafish were extracted from the Ensembl database. The zebrafish protein sequences were aligned with the corresponding proteins in different species by using ClustalW software (http://www.ebi.ac.uk/clustalw/).

The accession numbers for the *abca12* gene products in different species are: *E. caballus* (ENSECAP00000007797), *C. lupus familiaris* (XP_536058), *B. taurus* (XP_001788086), *H. sapiens* (NP_775099), *P. troglodytes* (XP_516070), *M. musculus* (XP_001002308), *R. norvegicus* (XP_237242), *G. gallus* (XP_421867), *D. rerio* (XP_686632) and *O. latipes* (ENSORLP00000020129). The accession numbers for *ABCC10* in *H. sapiens* is NP_258261. The accession numbers for *Abcc6* in different species are: *M. musculus* (NP_061265), *H. sapiens* (NP_001162), *D. rerio* (ENSDARP00000065432), *T. nigroviridis* (ENSTNIP00000015029) and *T. rubripes* (ENSTRUP00000029065).

The accession numbers for the *snap29* gene products in different species are: *H. sapiens* (NP_004773.1), *P. troglodytes* (XP_514997.2), *M. mulatta* (XP_001086227.1), *M. musculus* (NP_075837.3), *R. norvegicus* (NP_446262.3), *C. familiaris* (XP_543568.2), *B. taurus* (NP_001069427.1), *G. gallus* (NP_001025823.1), *D. rerio* (XP_700124.3), *S. salar* (NP_001134759.1), *X. laevis* (NP_001080076.1) and *A. thaliana* (NP_196405.1).

Phylogenetic analyses were conducted in the Molecular Evolution Genetics Analysis software (MEGA) version 4.0 (Tamura et al., 2007). The cladogram was constructed using the Neighbor-Joining method (Saitou and Nei, 1987). The Kimura two-parameter method was used to compute the evolutionary distances (Zuckerkandl and Pauling, 1965). The statistical reliance of NJ tree branches was evaluated using 1000 bootstrap samples.

For syntenic analysis, the orientation and chromosomal positions of *abca12* and *snap29* and their adjacent genes were determined manually from the gene orientations in the current Ensembl database. The zebrafish (Zv9), human (GRCh37/hg19), mouse (NCB137/mm9) and chicken (WUGSC2.1/galGal3) genome assembly versions were used for this analysis.

### In situ hybridization

Whole-mount in situ hybridization was performed as described previously (Thisse and Thisse, 2008). Collected zebrafish embryos were fixed in 4% paraformaldehyde before hybridization. Digoxigenin (DIG)-labeled antisense and sense probes were synthesized. After hybridization, detection was performed with an anti-DIG antibody coupled to alkaline phosphatase.

### Morpholinos and microinjection

Morpholino oligonucleotides were obtained from Gene Tools, LLC (Corvalis, OR). The morpholino oligomer sequences were written from 5′ to 3′, to correspond to the following genomic sequences (brackets surround the morpholino target sequence, exon sequences are capitalized, intron sequences are in lowercase, and nucleotide substitutions are bolded). For *abca12* knockdown: splice donor site morpholino (MO1), tgggaaataaatgtaatttacctgt, targets the exon-4–intron-4 junction, AAATGAAATAACTGA[ACAGgtaaattacatttatttccca]acggtc; 5-base pair mismatched control morpholino for *abca12* (cMO): tgg**c**aaa**a**aaat**c**taatttac**g**t**c**t. For *snap29* knockdown: splice donor site morpholino (MO2), ctgctcttgtgtttctcacccaggt, targets the exon-4–intron-4 junction,

GACAGAA[ACCTGGgtgagaaacacaagacag]cttctctcata; a second *snap29* splice junction morpholino (MO3) targets the intron 4-exon 5 border, ctcatctggaggacacaaacacaca, agtgtgtgtg[tgtgtg-tttgtgtcctccagATGAG]ATGTCTCTGGGTC. Global standard control morpholino (scMO), cctcttacctcagttacaatttata, has no target sequence in the zebrafish genome and is, therefore, inactive.

Embryos at the one- to four-cell stage were injected with an *abca12* morpholino (MO1, 25.6 ng) or *snap29* morpholinos (MO2, 2.6 ng and MO3, 5.2 ng) using glass microelectrodes fitted to a gas pressure injector (PL1-100, Harvard Apparatus). Electrodes were pulled (P-97, Flaming/Brown) and filled with morpholino and phenol red (final concentration 0.025%) to visualize the injected embryos. The embryos were then followed for viability, morphology and mRNA expression levels.

### Total RNA isolation and cDNA synthesis

Zebrafish embryos were collected at 0 as well as 6 hpf and 1-8 dpf. They were disintegrated by pipetting through a 21 gauge needle and total RNA was extracted using TRIzol reagent (Invitrogen, Carlsbad, CA). To remove contaminating genomic DNA, RNase-free DNase I digestion (Fisher Scientific, St Louis, MO) was performed. 1 μg of total RNA was reverse transcribed using the Superscript III First-Strand cDNA synthesis kit (Invitrogen) according to the manufacturer's protocol. Controls were performed by omitting the reverse transcriptase enzyme. All cDNA samples were stored at −20°C for future use.

### PCR amplification of cDNA

*abca12* cDNA was amplified by PCR using a forward primer on exon 4 (5′-ATCTGGGACAACTTGGGCAACT-3′), and a reverse primer on exon 5 (5′-TCATCTGGTCAGCAGTTCCAGAGA-3′). The *snap29* cDNA was amplified using a forward primer on exon 4 (5′-TTCTGCTGCTCTTGATAACGGCT-3′), and a reverse primer on exon 5 (5′-TTTAAGGCTTTTGAGCTGCCGGTT-3′). Primers for the zebrafish *β-actin* gene (fwd: 5′-ATCTGGCACCACACCTTCTACAATG; rev: 5′-GGGGTG-TTGAAGGTCTCAAACATGAT) were used as a positive control. PCR was performed using Taq polymerase and Q buffer (Qiagen, Valencia, CA), according to the manufacturer's instructions. The PCR conditions were as follows: an initial denaturation at 94°C for 5 minutes, followed by 35 cycles of 94°C for 1 minute; 58°C for 1 minute; 72°C for 1 minute; and finally 72°C for 10 minutes. The intensity of the bands was quantified using ImageQuant version 5.0 software (Molecular Dynamics, Sunnyvale, CA).

### mRNA rescue experiments

Capped full-length human mRNA corresponding to *ABCA12* was transcribed from an expression vector pCMV-Tag4B using the T3 mMessage mMachine kit (Ambion, Austin, TX). The morpholino was injected into one- to four-cell-stage embryos either alone or in combination with mRNA (2.3 ng) and followed for viability and morphology.

### Scanning electron microscopy

Samples were fixed in neutral buffered formalin at room temperature for 2 hours, followed by a rinse with phosphate buffered saline and an ethanol dehydration series of exchanges by completely replacing each successively higher ethanol solution with the next higher (20, 30, 50, 75, 95 and 100%). Samples were then incubated for 15 minutes in a 1.5 ml micro test tube containing 1,1,2-Trichloro-1,2,2-trifluoroethane before covering the open micro test tube with parafilm, punching holes in it with a 30G needle, and situating it under a fume hood where it was dried by turbulent air flow. Samples were then mounted onto stubs with carbon paint and coated in 50 nm of gold using a sputter coater. Specimens were imaged in a JEOL-T330A scanning electron microscope (JEOL, Tokyo, Japan) at 15 kV.

## TRANSLATIONAL IMPACT

### Clinical issue

Ichthyosis comprises a group of cutaneous disorders characterized by dry, scaly skin and a broad spectrum of other phenotypic manifestations. One of the most severe forms of ichthyosis is known as harlequin ichthyosis (HI); neonates affected with HI are born encased in a thick skin that restricts their movement and frequently die shortly after birth. Some forms of ichthyosis are syndromic; for example, CEDNIK syndrome is so-named because it consists of cerebral dysgenesis, neuropathy, ichthyosis and keratoderma. Details of the pathomechanisms of HI have recently been revealed through molecular genetics, which showed that patients with this disorder carry mutations in the *ABCA12* gene. Examination of *Abca12*$^{-/-}$ mice suggested that this gene encodes a transmembrane transporter present in the epidermis that is postulated to transport lipids (specifically ceramides) and that is required for formation of the stratum corneum on the surface of the skin. Although the mouse model is useful in that it recapitulates features of human HI, drawbacks include the long gestational period and the small number of offspring produced per litter. CEDNIK syndrome is caused by mutations in the *SNAP29* gene, which is required for normal vesicle trafficking and lipid transport in the epidermis. There is no animal model for this syndrome.

### Results

To create alternative, more expedient model systems to investigate pathological mechanisms of both HI and CEDNIK syndrome, the authors of this study knocked down the homologs of *ABCA12* and *SNAP29* in zebrafish embryos (*Danio rerio*). Morpholino antisense oligonucleotides targeted to exon-intron splice junctions were used to inhibit the splicing of *abca12* or *snap29* pre-mRNA. Inhibition of processing of either one of these mRNAs was accompanied by changes in the distribution of pigment along the trunk and tail of the fish as early as 2 days post-fertilization (dpf). Examination of epidermal morphology by scanning electron microscopy revealed perturbations in the surface contour of the keratinocytes, with loss of characteristic microridges and development of pathological spicules protruding from the center of each keratinocyte. These epidermal changes were accompanied by premature demise of the fish by 5 dpf. Transmission electron microscopy revealed an abundance of electron-dense granules in both morphants: lipid-like vesicles were seen in *abca12* knockdown fish, whereas the epidermis of *snap29* knockdown animals showed the presence of apparently empty vesicles.

### Implications and future directions

This study demonstrates that inhibition of *abca12* or *snap29* gene splicing in zebrafish leads to epidermal perturbations that are similar to those seen in human patients with various forms of ichthyosis. In addition, it suggests that interfering with two independent pathways involved in lipid transport can result in phenotypically similar perturbations in epidermal morphogenesis. These systems can serve as models to study ichthyosis, and provide a means to develop pharmacological approaches towards treatment of this currently intractable group of diseases. Finally, in a broader sense, this study attests to the feasibility of using zebrafish as a model system to study heritable skin diseases.

### Transmission electron microscopy

Samples were collected and fixed overnight at 4°C in 2.5% gluteraldehyde, 2% paraformaldehyde and 0.1 M sodium cacodylate. Samples were then washed in 0.1 M sodium cacodylate before undergoing secondary fixation in 2% osmium tetroxide, 1.5% potassium ferricyanide and 0.1 M sodium. Samples were again washed with 0.1 M sodium cacodylate followed by deionized water before undergoing en block staining with 2% uranyl acetate. Samples were washed again with deionized water, then dehydrated in a graded ethanol series and embedded in EMbed-812 (EMS, Hatfield, PA). Ultrathin sections (60 nm) were cut and analyzed using a JEOL JEM-1010 transmission electron microscope fitted with a Hamamatsu digital camera (Hamamatsu Photonics, Hamamatsu City, Japan) and AMT Advantage image capture software (AMT, Danvers, MA).

### Statistical analysis

Risk differences and 95% confidence intervals were calculated between experimental groups with regards to survival, skin phenotype and edema in Table 1, for 3 dpf and 5 dpf separately. Fisher's exact test was used to determine the difference between proportions because of the presence of cells with zero observations. Adjustments for multiple comparisons were performed using False Discovery Rate, and it is these adjusted *P*-values that are reported. Analyses were conducted using SAS 9.2 (SAS Institute, Cary, NC).

#### ACKNOWLEDGEMENTS

The authors thank the following colleagues for advice and assistance: Wolfgang Driever, Institute for Biology I, University of Freiburg; Raymond Meade, Biomedical Imaging Core Facility, University of Pennsylvania; Gerald Harrison, Department of Biochemistry, School of Dental Medicine, University of Pennsylvania; Jean-Yves Sire, Equipe "Evolution et Développement du Squelette", Université Paris; Eijiro Adachi, Department of Matrix Biology and Tissue Regeneration, Graduate School of Medical Sciences, Kitasato University; Ulrich Rodeck, Gabor Kari, April Aguillard, Adele Donahue and Andrzej Fertala, Department of Dermatology and Cutaneous Biology, Thomas Jefferson University; Terry Hyslop and Jocelyn Andrel, Department of Pharmacology and Experimental Therapeutics, Thomas Jefferson University. Carol Kelly assisted in manuscript preparation. This study was supported by the NIH/NIAMS grant R01AR055225 to J.U.; by the University of Virginia to C.T. and B.T. Q.L. is a recipient of a Research Career Development Award from the Dermatology Foundation.

#### COMPETING INTERESTS

The authors declare that they do not have any competing or financial interests.

#### AUTHOR CONTRIBUTIONS

Q.L., M.F., C.T. and B.T. performed the experiments; M.A. provided reagents; H.S. and E.S. interpreted the data and edited the manuscript; S.-Y.H. contributed to the data analysis; J.U. developed the concept, interpreted the data and prepared the manuscript.

#### REFERENCES

**Akiyama, M.** (2006a). Harlequin ichthyosis and other autosomal recessive congenital ichthyoses: the underlying genetic defects and pathomechanisms. *J. Dermatol. Sci.* **42**, 83-89.

**Akiyama, M.** (2006b). Pathomechanisms of harlequin ichthyosis and ABCA transporters in human diseases. *Arch. Dermatol.* **142**, 914-918.

**Akiyama, M.** (2010). *ABCA12* mutations in harlequin ichthyosis, congenital ichthyosiform erythroderma and lamellar ichthyosis. *Hum. Mutat.* **31**, 1090-1096.

**Akiyama, M., Sugiyama-Nakagiri, Y., Sakai, K., McMillan, J. R., Goto, M., Arita, K., Tsuji-Abe, Y., Tabata, N., Matsuoka, K. and Sasaki, R.** (2005). Mutations in lipid transporter ABCA12 in harlequin ichthyosis and functional recovery by corrective gene transfer. *J. Clin. Invest.* **115**, 1777-1784.

**Brown, S. J. and Irvine, A. D.** (2008). Atopic eczema and the filaggrin story. *Semin. Cutan. Med. Surg.* **27**, 128-137.

**Brown, S. J. and McLean, W. H. I.** (2008). Eczema genetics: current state of knowledge and future goals. *J. Invest. Dermatol.* **129**, 543-552.

**Elias, P. M., Crumrine, D., Rassner, U., Hachem, J. P., Menon, G. K., Man, W., Choy, M. H., Leypoldt, L., Feingold, K. R. and Williams, M. L.** (2004). Basis for abnormal desquamation and permeability barrier dysfunction in RXLI. *J. Invest. Dermatol.* **122**, 314-319.

**Fuchs-Telem, D., Stewart, H., Rapaport, D., Nousbeck, J., Gat, A., Gini, M., Lugassy, Y., Emmert, S., Eckl, K., Hennies, H. C. et al.** (2011). CEDNIK syndrome results from loss-of-function mutations in SNAP29. *Br. J. Dermatol.* **164**, 610-616.

**Fukazawa, C., Santiago, C., Park, K. M., Deery, W. J., Gomez de la Torre Canny, S., Holterhoff, C. K. and Wagner, D. A.** (2010). poly/chuk/ikk1 is required for differentiation of the zebrafish embryonic epidermis. *Dev. Biol.* **346**, 272-283.

**Kaminski, W. E., Piehler, A. and Wenzel, J. J.** (2006). ABC A-subfamily transporters: structure, function and disease. *Biochim. Biophys. Acta* **1762**, 510-524.

**Kari, G., Rodeck, U. and Dicker, A. P.** (2007). Zebrafish: an emerging model system for human disease and drug discovery. *Clin. Pharmacol. Ther.* **82**, 70-80.

**Kelsell, D. P., Norgett, E. E., Unsworth, H., Teh, M. T., Cullup, T., Mein, C. A., Dopping-Hepenstal, P. J., Dale, B. A., Tadini, G. and Fleckman, P.** (2005). Mutations in ABCA12 underlie the severe congenital skin diseases harlequin ichthyosis. *Am. J. Hum. Genet.* **76**, 794-803.

**Kimmel, C. B., Ballard, W. W., Kimmel, S. R., Ullmann, B. and Schilling, T. F.** (1995). Stages of embryonic development of the zebrafish. *Dev. Dyn.* **203**, 253-310.

**Le Guellec, D., Morvan-Dubois, G. and Sire, J. Y.** (2004). Skin development in bony fish with particular emphasis on collagen deposition in the dermis of the zebrafish (Danio rerio). *Int. J. Dev. Biol.* **48**, 217-232.

**Lefèvre, C., Audebert, S., Jobard, F., Bouadjar, B., Lakhdar, H., Boughdene-Stambouli, O., Blanchet-Bardon, C., Heilig, R., Foglio, M. and Weissenbach, J.** (2003). Mutations in the transporter ABCA12 are associated with lamellar ichthyosis type 2. *Hum. Mol. Genet.* **12**, 2369-2378.

**Li, Q., Frank, M., Thisse, C., Thisse, B. and Uitto, J.** (2011). Zebrafish: a model system to study heritable skin diseases. *J. Invest. Dermatol.* **131**, 565-571.

**McGrath, J. A. and Uitto, J.** (2008). The filaggrin story: novel insights into skin-barrier function and disease. *Trends Mol. Med.* **14**, 20-27.

**Montpetit, A., Côté, S., Brustein, E., Drouin, C. A., Lapointe, L., Boudreau, M., Meloche, C., Drouin, R., Hudson, T. J., Drapeau, P. et al.** (2008). Disruption of AP1S1, causing a novel neurocutaneous syndrome, perturbs development of the skin and spinal cord. *PloS Genet.* **4**, e1000296.

**Rapaport, D., Lugassy, Y., Sprecher, E. and Horowitz, M.** (2010). Loss of SNAP29 impairs endocytic recycling and cell motility. *PloS ONE* **5**, e9759.

**Sabel, J. L., d'Alençon, C., O'Brien, E. K., Van Otterloo, E., Lutz, K., Cuykendall, T. N., Schutte, B. C., Houston, D. W. and Cornell, R. A.** (2009). Maternal interferon regulatory factor 6 is required for the differentiation of primary superficial epithelia in Danio and Xenopus embryos. *Dev. Biol.* **325**, 249-263.

**Saitou, N. and Nei, M.** (1987). The neighbor-joining method: a new method for reconstructing phylogenetic trees. *Mol. Biol. Evol.* **4**, 406-425.

**Sakai, K., Akiyama, M., Sugiyama-Nakagiri, Y., McMillan, J. R., Sawamura, D. and Shimizu, H.** (2007). Localization of ABCA12 from golgi apparatus to lamellar granules in human upper epidermal keratinocytes. *Exp. Dermatol.* **16**, 920-926.

**Slanchev, K., Carney, T. J., Stemmler, M. P., Koschorz, B., Amsterdam, A., Schwarz, H. and Hammerschmidt, M.** (2009). The epithelial cell adhesion molecule EpCAM is required for epithelial morphogenesis and integrity during zebrafish epiboly and skin development. *PLoS Genet.* **5**, e1000563.

**Smyth, I., Hacking, D. F., Hilton, A. A., Mukhamedova, N., Meikle, P. J., Ellis, S., Satterley, K., Collinge, J. E., de Graaf, C. A. and Bahlo, M.** (2008). A mouse model of harlequin ichthyosis delineates a key role for Abca12 in lipid homeostasis. *PLoS Genet.* **4**, e1000192.

**Sprecher, E., Ishida-Yamamoto, A., Mizrahi-Koren, M., Rapaport, D., Goldsher, D., Indelman, M., Topaz, O., Chefetz, I., Keren, H., O'Brien, T. J. et al.** (2005). A mutation in SNAP29, coding for a SNARE protein involved in intracellular trafficking, causes a novel neurocutaneous syndrome characterized by cerebral dysgenesis, neuropathy, ichthyosis, and palmoplantar keratoderma. *Am. J. Hum. Genet.* **77**, 242-251.

**Sundberg, J. P., Boggess, D., Hogan, M. E., Sundberg, B. A., Rourk, M. H., Harris, B., Johnson, K., Dunstan, R. W. and Davisson, M. T.** (1997). Harlequin ichthyosis (ichq): a juvenile lethal mouse mutation with ichthyosiform dermatitis. *Am. J. Pathol.* **151**, 293-310.

**Tamura, K., Dudley, J., Nei, M. and Kumar, S.** (2007). MEGA4: molecular evolutionary genetics analysis (MEGA) software version 4.0. *Mol. Biol. Evol.* **24**, 1596-1599.

**Thisse, C. and Thisse, B.** (2008). High resolution in situ hybridization on whole-mount zebrafish embryo. *Nat. Protoc.* **3**, 59-69.

**Tusnády, G. E., Sarkadi, B., Simon, I. and Váradi, A.** (2006). Membrane topology of human ABC proteins. *FEBS Lett.* **580**, 1017-1022.

**Yanagi, T., Akiyama, M., Nishihara, H., Sakai, K., Nishie, W., Tanaka, S. and Shimizu, H.** (2008). Harlequin ichthyosis model mouse reveals alveolar collapse and severe fetal skin barrier defects. *Hum. Mol. Genet.* **17**, 3075-3083.

**Zuckerkandl, E. and Pauling, L.** (1965). Evolutionary divergence and convergence in proteins. In *Evolving Genes and Proteins* (ed. V. Bryson and H. J. Vogel), pp. 97-166. New York: Academic Press.

thickness of the mucous layer of small intestines, resulting in the inhibition of small intestinal absorption.[4] In addition, PGE1 increases blood flow in the stomach and upregulates the digestion in the stomach. During the provocation test in our case, serum gliadin levels were not increased by administering misoprostol. However, sodium cromoglicate, a mast cell stabilizer commonly used to treat allergic rhinitis, allergic conjunctivitis, and asthma, could not affect serum gliadin levels in the provocation test, and therefore allowed the symptoms to occur. We consider that the effects of misoprostol on the alimentary tract are crucial for the prevention of FDEIA. Our observation indicates that the exacerbating effect of aspirin in FDEIA comes from the inhibitory effects of aspirin on PGE1 in the gastrointestinal milieu. Thus, misoprostol would be a promising prophylactic drug for FDEIA.

*Aya Takahashi,* MD
*Kimiko Nakajima,* MD
*Mitsunori Ikeda,* MD
*Shigetoshi Sano,* MD
Department of Dermatology
Kochi Medical School, Nankoku
Kochi
Japan

*Kunie Kohno,* MD
*Eishin Morita,* MD
Department of Dermatology
Shimane University Faculty of Medicine
Izumo, Shimane
Japan
E-mail: jm-aya.derm@kochi-u.ac.jp

*References*

1 Matsuo H, Morita E, Tatham AS, *et al.* Identification of the IgE-binding epitope in omega-5 gliadin, a major allergen in wheat-dependent exercise-induced anaphylaxis. *J Biol Chem* 2004; 279: 12135–40.
2 Matsuo H, Morimoto K, Akaki T, *et al.* Exercise and aspirin increase levels of circulating gliadin peptides in patients with wheat-dependent exercise-induced anaphylaxis. *Clin Exp Allergy* 2005; 35: 461–6.
3 Sheffer AL, Tong AK, Murphy GF, *et al.* Exercise-induced anaphylaxis: a serious form of physical allergy associated with mast cell degranulation. *J Allergy Clin Immunol* 1985; 75: 479–84.
4 Gurleyik E, Coskun O, Ustundag N, *et al.* Prostaglandin E1 maintains structural integrity of intestinal mucosa and prevents bacterial translocation during experimental obstructive jaundice. *J Invest Surg* 2006; 19: 283–9.

**Type XVII collagen ELISA indices significantly decreased after bullous pemphigoid remission**

The major pathogenic epitope of bullous pemphigoid (BP) is known to be the noncollagenous extracellular domain (NC16A) of type XVII collagen (COL17).[1] Here we investigated indirect immunofluorescence (IIF) and COL17 NC16A domain enzyme-linked immunosorbent assay (ELISA)[2–5] data before treatment and after remission to evaluate the usefulness of ELISA analyses as indicators for BP disease activity.

We included ten consecutive BP patients [eight women and two men: between 33 and 80 years old (mean; 59 years old)] who showed typical clinical features before treatment and were successfully treated, resulting in complete or partial remission at our institute. The first day of each patient visit was within the last three years. In all patients, the diagnosis was confirmed by histopathological observation and immunofluorescence study, i.e. histopathological subepidermal blister formation was observed and direct and IIF studies revealed the presence of autoantibodies along the dermal–epidermal junction. All patients were successfully treated with oral prednisolone therapy of 30–50 mg/d with or without azathioprine or a combination therapy using tetracycline and nicotinamide. Treatment periods from initial diagnosis to remission ranged from four months to 35 months (mean; 14.6 ± 10.8 months). Serum samples were obtained for ELISA and IIF at least twice during the disease course for each patient.

Concentration of autoantibodies in the patients' sera directed against the NC16A domain of COL17 was measured using the COL17 NC16A ELISA kit following the kit's instructions.[6] IIF staining and evaluation were performed as previously described using normal human skin as a substrate.[7]

In all the cases, the ELISA indices showed a decrease during the successful treatment course. ELISA indices after remission were significantly reduced compared with those before treatment ($P < 0.0001$) (Fig. 1a). IIF titers also decreased after remission in six cases, but the titers were not apparently reduced in the other four cases, although a statistically significant reduction in combined IIF titer was observed after remission compared with those before treatment ($P < 0.05$) (Fig. 1b).

Positive correlation between ELISA indices and BP disease activity has been reported previously in the literature. Di Zenzo *et al.*[8] demonstrated that disease severity before treatment was well correlated with ELISA indices in BP patients. Izumi *et al.*[9] described ELISA indices and alteration of disease activity of five BP patients during various treatments. In this study, we compared the ELISA

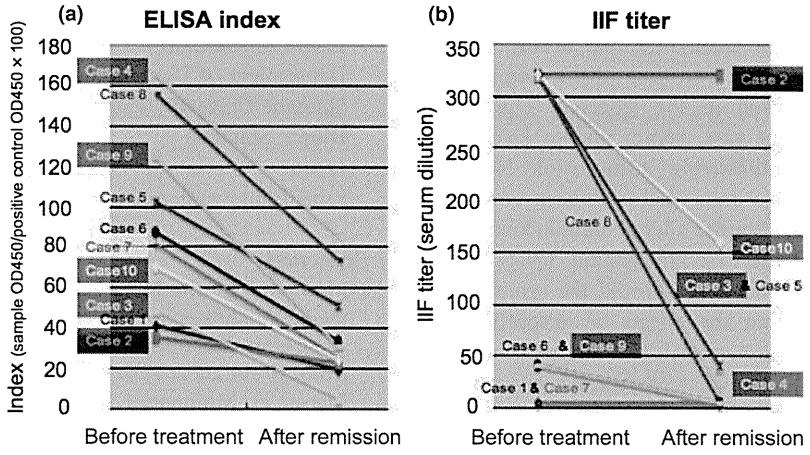


**Figure 1** ELISA indices and indirect immunofluorescence (IIF) titers before treatment and after remission. (a) ELISA indices of successfully treated BP patients. Disease remission was defined as when erythema, bullae and erosions had completely healed (complete remission) or no more than three bullae or erythema were seen in a week (partial remission) and only a low dose of oral prednisolone (<5 mg/d) or no treatment was needed to maintain this condition. As ELISA indices after remission, we adopted ELISA indices at the time when each patient's disease activity was evaluated as being in "complete remission" or "partial remission" (as defined above) for the first time after treatment. Mean ELISA index of the 10 patients before treatment was 91.3 ± 45.7 (range: 35.6–165.6) and the mean index after remission was 37.4 ± 25.3 (range: 6.0–86.4). After complete or partial remission, the ELISA indices were significantly reduced ($P < 0.0001$). (b) IIF titers of the same patients. Apparent decreases in IIF titers after remission were seen only in six patients. Mean IIF titer of the 10 patients before treatment was 201 ± 154 (range: 5–320) and the mean titer after remission was 60.5 ± 102.8 (range: 5–320). A statistically, significant reduction was observed in combined IIF titers after remission compared with those before treatment ($P < 0.05$). Colors of the lines are specific for each patient in both figures (a) and (b)

indices before treatment and after remission in our BP patient cohort and clearly demonstrated that ELISA indices significantly decreased after remission. Feng *et al.*[10] reported similar results on correlation of ELISA indices with disease course in BP patients, although the time points for ELISA after treatment were just before the decrease in corticosteroid and when the dosage of corticosteroid was successfully decreased to half the initial dose in the report. In this study, we employed ELISA indices at the time when each patient's disease activity was evaluated as "complete remission" or "partial remission" for the first time after treatment. Thus, this study is unique in the point that we evaluated exact correlation between ELISA indices and disease remission.

In conclusion, the present results further support the idea that the COL17 NC16A ELISA indices demonstrate a correlation with the BP disease remission more accurately than IIF titers and are a useful tool to detect BP disease remission and to assess the efficacy of BP treatment.

*Erika Kusajima*
*Masashi Akiyama,* MD, PhD
*Megumi Sato*
*Ken Natsuga,* MD
*Hiroshi Shimizu,* MD, PhD
Department of Dermatology
Hokkaido University Graduate School of Medicine
Sapporo
Japan
E-mail: akiyama@med.hokudai.ac.jp
Conflict of interest: the authors state no conflict of interest.

*References*

1 Giudice GJ, Emery DJ, Zelickson BD, *et al.* Bullous pemphigoid and herpes gestationis autoantibodies recognize a common non-collagenous site on the BP180 ectodomain. *J Immunol* 1993; 151: 5742–5750.
2 Zillikens D, Mascaro JM, Rose PA, *et al.* A highly sensitive enzyme-linked immunosorbent assay for the detection of circulating anti-BP180 autoantibodies in patients with bullous pemphigoid. *J Invest Dermatol* 1997; 109: 679–683.
3 Hata Y, Fujii Y, Tsunoda K, Amagai M. Production of the entire extracellular domain of BP180 (type XVII collagen) by baculovirus expression. *J Dermatol Sci* 2000; 23: 183–190.
4 Schmidt E, Obe K, Brocher EB, Zillikens D. Serum levels of autoantibodies to BP180 correlate with disease activity in patients with bullous pemphigoid. *Arch Dermatol* 2000; 136: 174–178.

5 Kobayashi M, Amagai M, Kuroda-Kinoshita K, *et al.* BP180 ELISA using bacterial recombinant NC16a protein as a diagnostic and monitoring tool for bullous pemphigoid. *J Deramtol Sci* 2002; 30: 224–232.
6 Tsuji-Abe Y, Akiyama M, Yamanaka Y, *et al.* Correlation of clinical severity and ELISA indices for the NC16A domain of BP180 measured using BP180 ELISA kit in bullous pemphigoid. *J Dermatol Sci* 2005; 37: 145–149.
7 Beutner EH, Jordon RE, Chorzelski TP. The immunopathology of pemphigus and bullous pemphigoid. *J Invest Dermatol* 1968; 51: 63–80.
8 Di Zenzo G, Thoma-Uszynski S, Fontao L, *et al.* Multicenter prospective study of the humoral autoimmune response in bullous pemphigoid. *Clin Immunol* 2008; 128: 415–426.
9 Izumi T, Ichiki Y, Esaki C, Kitajima Y. Monitoring of ELISA for anti-BP180 antibodies: clinical and therapeutic analysis of steroid-treated patients with bullous pemphigoid. *J Dermatol* 2004; 31: 383–391.
10 Feng S, Wu Q, Jin P, *et al.* Serum levels of autoantibodies to BP180 correlate with disease activity in patients with bullous pemphigoid. *Int J Dermatol* 2008; 47: 225–228.

prednisolone in HIV-infected individuals. J Acquir Immune Defic Syndr 2008;48:561-6.
5. Dort K, Padia S, Wispelwey B, Moore CC. Adrenal suppression due to an interaction between ritonavir and injected triamcinolone: a case report. AIDS Res Ther 2009;6:10.

doi:10.1016/j.jaad.2010.09.014

## Subepidermal blistering disease with 3 distinct autoantibodies: Anti-BP230, anti-laminin gamma-1, and anti-laminin-332

*To the Editor:* A 25-year-old Japanese woman presented with pruritic tense blisters involving the lips, forearms, fingers, and soles (Fig 1, *A-C*). No mucosal involvement was observed. A skin biopsy specimen taken from a bulla on her left forearm demonstrated subepidermal separation with eosinophilic inflammatory infiltrate in the dermis (Fig 2, *A*). Direct immunofluorescence (IF) microscopy of the lesion showed linear deposition of C3 and IgG at the dermoepidermal junction (Fig 2, *B* and *C*). Indirect IF on sodium-split skin revealed linear IgG deposition on both the epidermal and the dermal sides (titer 1:20; Fig 2, *D*). Enzyme-linked immunosorbent assay (ELISA) using bacterial recombinant protein of the NC16a domain of COL17 (MBL, Nagoya, Japan) was negative. ELISA using bacterial recombinant proteins of the N- and C-terminal domains of BP230 (MBL, Nagoya, Japan) was also negative. Immunoblot analysis with epidermal and dermal extracts derived from normal human skin and purified laminin-332 was performed. The results showed the presence of circulating IgG autoantibodies against BP230, laminin $\gamma$1, and the $\gamma$ 2 chain of laminin-332 (Fig 2, *E, F,* and *G*). Oral prednisolone, 40 mg per day (PSL), failed to alleviate the symptoms. With the addition of 75 mg per day of oral diaphenylsulfone (DDS), the cutaneous lesions rapidly healed with postinflammatory hyperpigmentation. PSL and DDS were tapered without relapse of skin lesions. At 10 months after referral, she discontinued PSL and was taking DDS at 25 mg daily.

Previously, antibodies against laminin-332 were detected in about 10% to 20% of mucous membrane pemphigoid (MMP) patients. The majority of the patients have antibodies reactive with the $\alpha$3 subunit of the protein. However, our case showed reactivity only with the $\gamma$2 subunit. The mucosal involvement that is typically seen in MMP was not observed in our case.

Circulating antibodies against BP230 were detected in the serum of a patient by immunoblot analysis but not by BP230 ELISA (MBL, Nagoya, Japan). This ELISA system utilizes the N- and C-terminal domains of BP230, but not the central-rod domain.[1] Therefore the autoantibodies against BP230 that were detected in our immunoblot study may have reacted with the central-rod domain of the BP230 antigen. Autoantibodies against BP230, an intracellular protein, are clearly associated with bullous pemphigoid (BP), but have not been shown to be involved in the initiation of the disease. A marked improvement with the administration of DDS and the absence of erythematous plaques in the patient were not typical of the BP clinical course and manifestations.

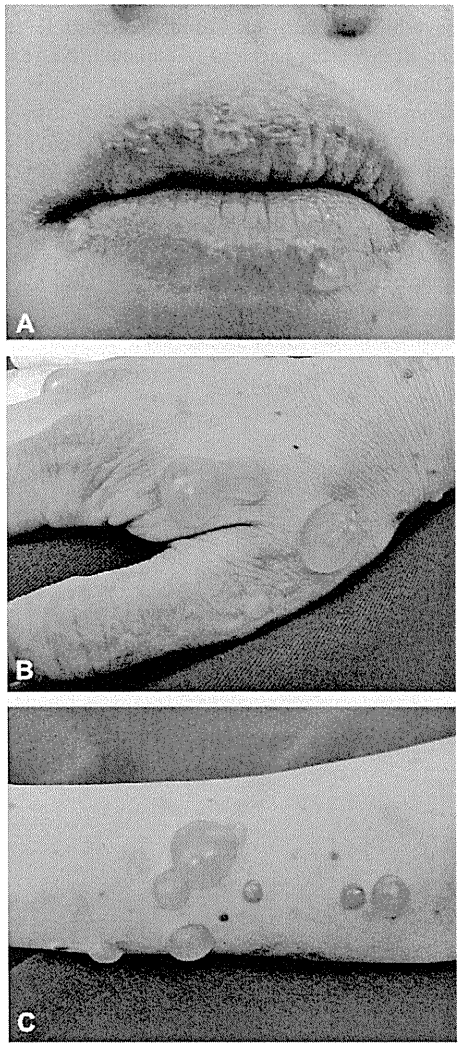


**Fig 1.** Clinical presentation of the patient. Tense blisters involve the fingers (**A**), forearms (**B**), and lips (**C**).

Autoantibodies against laminin $\gamma$1 are characteristic of anti-laminin $\gamma$1 pemphigoid.[2] Blisters involving the lips and therapeutic improvement with DDS are compatible with the clinical features of anti-laminin $\gamma$1 pemphigoid. On the basis of these findings, the diagnosis of anti-laminin $\gamma$1 pemphigoid may be appropriate.

It is possible that the unusual autoimmune profile of the patient developed as a result of epitope

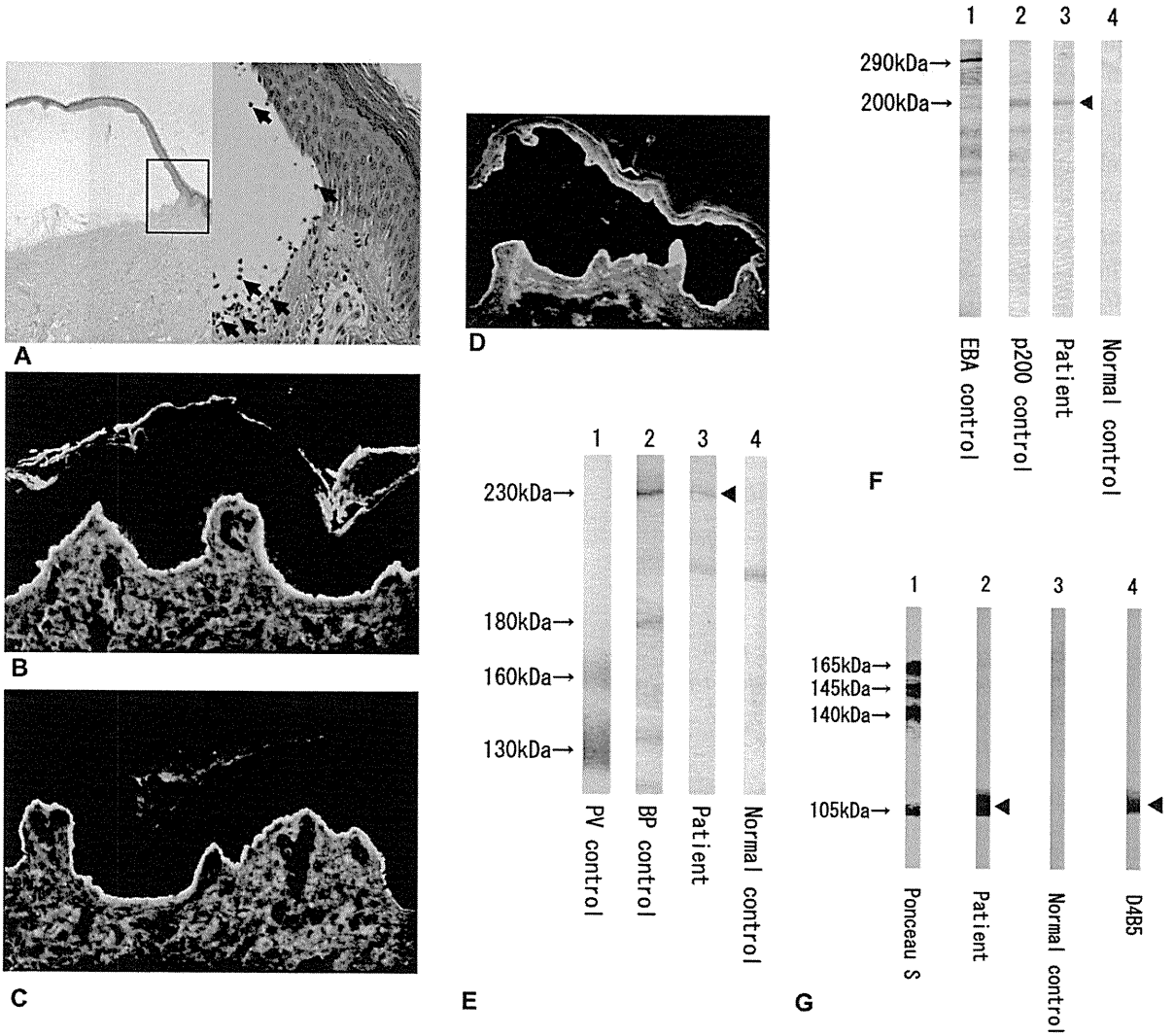


**Fig 2.** Histologic examination of skin specimens from patient's left forearm. **A**, Hematoxylin-eosin stain. Subepidermal blister (original magnification: ×40) with infiltration of eosinophils (*arrows*) in blister cavity (×200). Direct immunofluorescence of perilesional skin samples shows linear deposition of C3 (**B**) and IgG (**C**) at the dermoepidermal junction (×40). Immunological characterization of autoantibodies. **D**, Indirect immunofluorescence on 1M NaCl-split skin. Circulating IgG antibodies bind to both epidermal and dermal sides (titer 1:20). **E**, Immunoblot analysis using human epidermal extracts. *Lane 1*: A reference BP serum reacting with 180-kd (COL17) and 230-kd (BP230) antigens. *Lane 2*: A reference pemphigus vulgaris serum with positive bands at 130 kd (Dsg3) and 160 kd (Dsg1). *Lane 3*: Patient's serum. IgG in patient's serum reacts with BP230. **F**, Immunoblot analysis using human dermal extracts. *Lane 1*: A reference EBA serum reacting with a 290-kd molecule (type VII collagen). *Lane 2*: A reference anti-laminin γ1 pemphigoid serum with a positive band at 200 kd (p200, laminin γ1). *Lane 3*: Patient's serum. *Lane 4*: A reference normal serum. IgG in patient's serum reacts with 200-kd antigen. **G**, Immunoblot analysis using purified laminin-332 (courtesy of Dr S. Amano, Shiseido Life Science Research Center, Yokohama, Japan). *Lane 1*: A reference of Ponceau S stain of laminin-332 consisting of α3 (165 kd, 145 kd), β3 (140 kd), and γ2 (105 kd) subunits. *Lane 2*: Patient's serum. *Lane 3*: A reference normal serum. *Lane 4*: A reference of D4B5 (Millipore, Bedford, MA), a mouse monoclonal antibody against the γ2 subunit of laminin-332. IgG from patient's serum and D4B5 reacts with the γ2 subunit of laminin-332 (105 kd).

spreading. Although several cases of autoimmune blistering disease with distinct autoantigens have been reported,[3-5] to our knowledge this is the first case report describing a patient with IgG autoantibodies for three different antigens to the basement membrane zone: BP230, laminin $\gamma 1$ and the $\gamma 2$ subunit of laminin-332.

*Kazuhiro Kikuchi, MD, PhD,[a,b] Ken Natsuga, MD, PhD,[b] Satoru Shinkuma, MD,[b] Wataru Nishie, MD, PhD,[b] Satoshi Kajita, MD, PhD,[c] Hidetsugu Sato, MD, PhD,[a] and Hiroshi Shimizu, MD, PhD[b]*

*Department of Dermatology, Obihiro Kosei General Hospital, Obihiro[a]; Department of Dermatology, Hokkaido University Graduate School of Medicine, Sapporo[b]; and Takagi Dermatology Clinic, Obihiro,[c] Japan*

*Funding sources: None.*

*Conflicts of interest: None declared.*

*Reprint requests: Ken Natsuga, MD, PhD, Department of Dermatology, Hokkaido University Graduate School of Medicine, N15 W7, Sapporo 060-8638, Japan*

*E-mail: natsuga@med.hokudai.ac.jp*

**REFERENCES**

1. Yoshida M, Hamada T, Amagai M, Hashimoto K, Uehara R, Yamaguchi K, et al. Enzyme-linked immunosorbent assay using bacterial recombinant proteins of human BP230 as a diagnostic tool for bullous pemphigoid. J Dermatol Sci 2006;41:21-30.
2. Dainichi T, Kurono S, Ohyama B, Ishii N, Sanzen N, Hayashi M, et al. Anti-laminin gamma-1 pemphigoid. Proc Natl Acad Sci U S A 2009;106:2800-5.
3. Izumi R, Fujimoto M, Yazawa N, Nakashima H, Asashima N, Watanabe R, et al. Bullous pemphigoid positive for anti-BP180 and anti-laminin 5 antibodies in a patient with graft-vs-host disease. J Am Acad Dermatol 2007;56:94-7.
4. Shimanovich I, Petersen EE, Weyers W, Sitaru C, Zillikens D. Subepidermal blistering disease with autoantibodies to both the p200 autoantigen and the alpha3 chain of laminin 5. J Am Acad Dermatol 2005;52:90-2.
5. Mitsuya J, Hara H, Ito K, Ishii N, Hashimoto T, Terui T. Metastatic ovarian carcinoma-associated subepidermal blistering disease with autoantibodies to both the p200 dermal antigen and the gamma 2 subunit of laminin 5 showing unusual clinical features. Br J Dermatol 2008;158:1354-7.

doi:10.1016/j.jaad.2010.09.719

## Thrombosis-induced ulcerations of the lower legs with coexistent anetoderma due to antithrombin III deficiency

*To the Editor:* A 54-year-old white man with schizoaffective disorder and insulin-dependent diabetes mellitus presented with a several-month history of nonhealing, painful ulcerations of the lower extremities. On examination, the right lower extremity had a 10- × 6-cm ulcer with irregular borders. Closer observation revealed numerous flesh-colored, atrophic 1- to 2-cm plaques on skin surrounding the ulceration consistent with anetoderma (Fig 1). These lesions were asymptomatic and began concomitantly with ulcer development. Livedo reticularis was not present. Initial evaluation included a biopsy of the ulceration and laboratory investigation for hereditary and acquired hypercoagulable states. Histologic evaluation of the ulceration revealed deep and superficial thromboses with prominent overlying infarct, without evidence of primary vasculitis or pyoderma gangrenosum. Laboratory evaluation for anti-phospholipid antibodies and cryoglobulins were negative; however, anti-thrombin III activity was reduced. Repeat testing revealed below normal antithrombin III activity (mean, 74%; normal, 80%-120%) and reduced antigen level at 19.6% (normal, 22%-36%). A Doppler ultrasound of the lower extremities was negative for deep vein thrombosis.

**Fig 1.** Lesions of anetoderma surrounding thrombotic-induced ulceration on right leg.

The patient was referred to the hematology service; a trial of coagulation prophylaxis with enoxaparin (Lovenox, Sanofi-Aventis), 40 mg administered subcutaneously twice daily, was performed. This resulted in complete resolution of all skin lesions over several weeks (Fig 2). Several weeks later, the patient presented with recurrence of lower extremity ulcerations. It was discovered that the patient had self-discontinued treatment with enoxaparin because of pain with medication injection as well as cutaneous bleeding and bruising with minimal trauma. Subsequent replacement with fondaparinux (Arixtra, Glasko Smith Kline, Brentford,